

A HIGHLY ACCURATE BOUNDARY INTEGRAL METHOD FOR THE ELASTIC OBSTACLE SCATTERING PROBLEM

HEPING DONG, JUN LAI, AND PEIJUN LI

ABSTRACT. Consider the scattering of a time-harmonic plane wave by a rigid obstacle embedded in a homogeneous and isotropic elastic medium in two dimensions. In this paper, a novel boundary integral formulation is proposed and its highly accurate numerical method is developed for the elastic obstacle scattering problem. More specifically, based on the Helmholtz decomposition, the model problem is reduced to a coupled boundary integral equation with singular kernels. A regularized system is constructed in order to handle the degenerated integral operators. The semi-discrete and full-discrete schemes are studied for the boundary integral system by using the trigonometric collocation method. Convergence is established for the numerical schemes in some appropriate Sobolev spaces. Numerical experiments are presented for both smooth and nonsmooth obstacles to demonstrate the superior performance of the proposed method.

1. INTRODUCTION

The phenomena of elastic scattering by obstacles have received ever-increasing attention due to the significant applications in diverse scientific areas such as geological exploration, nondestructive testing, and medical diagnostics [3, 21]. The scattering problems for elastic waves have been extensively studied; there are many mathematical and computational results available for both the direct and inverse scattering problems [1, 12, 22, 25, 27]. It has played an important role to have an accurate and efficient numerical method in many of these applications since a large number of forward simulations are often required. Due to the coexistence of compressional and shear wave components with different wavenumbers, the propagation of elastic waves governed by the Navier equation is much more complicated than that of acoustic waves governed by the Helmholtz equation. This paper is concerned with the scattering of a time-harmonic plane wave by a rigid obstacle embedded in a homogeneous and isotropic elastic medium in two dimensions. We propose a novel boundary integral formulation and develop a highly accurate numerical method for solving the elastic obstacle scattering problem.

Given the importance of elasticity, various numerical methods have been proposed to solve the associated scattering problems in the literature. Conventional methods include the finite difference and finite element methods. Despite being successful to deal with media with general properties and geometries, they require the discretization of the whole computational domain and encounter the issue of domain truncation by adding some artificial absorbing boundary layers [10]. The method of boundary integral equations offers an attractive alternative for solving the exterior boundary value problems such as the obstacle scattering problems. It only requires the discretization of boundary of the domain and satisfies the radiation condition exactly [25], but it does require the knowledge of Green's function for the governing equation. As is known, the Green function of the elastic wave equation is a second order tensor and is complicated to be applied in the computation of boundary integral equations. Readers are referred to [5, 6] and reference therein for some recent advances along this direction. To bypass this complexity, we introduce two scalar potential functions and use the Helmholtz decomposition to split the displacement of the elastic wave field into the compressional

2010 *Mathematics Subject Classification.* 65N38, 65R20, 45L05, 45P05.

Key words and phrases. elastic wave scattering, boundary integral equation, collocation method, Helmholtz decomposition, convergence analysis.

wave and the shear wave. The two wave components, both of which satisfy the two-dimensional Helmholtz equation [8, 20, 28], are only coupled at the boundary of obstacle. Therefore, the boundary value problem of the Navier equation is converted equivalently into a coupled boundary value problem of the Helmholtz equations for the potentials. Compared to the formulation based on the second order tensor elastic Green's function, such a decomposition reduce greatly the complexity for the computation of the elastic scattering problem. Similar techniques have also been successfully applied to the equations of unsteady and incompressible flow [11].

Another goal of this work is to carry on the convergence analysis of a high order numerical discretization for the boundary integral system. Numerical discretization for boundary integral equations requires special quadratures due to singular integral kernels [2]. The quadrature methods for the logarithmic and hypersingular integral equations were proposed in [16, 19] to solve the sound-soft and sound-hard obstacle scattering problems, where the error analysis was done in the Sobolev space and Hölder space, respectively. As an improvement of the quadrature method for the sound-hard obstacle scattering problem, based on the trigonometric differentiation to discrete the principal part of the hypersingular operator, a fully discrete collocation method was proposed in [17] and the convergence in a Sobolev space setting was also proven. In [26], the authors showed an error analysis by using the trigonometric collocation method for the boundary integral equation which contains more general singular integral operators. A Galerkin boundary element method with a regularization for the hypersingular integral was developed in [5] to solve the two-dimensional elastic scattering problem. In [14], the problem for bending of an elastic plate with the Dirichlet boundary conditions was studied. An explicit equivalent regularizer was constructed for the Fredholm integral equation of second kind to derive existence and uniqueness results in an appropriate Sobolev space. A high order spectral algorithm was developed in [23] for the three-dimensional elastic obstacle scattering problem with the Dirichlet or Neumann boundary condition. A Nyström method with a local correction scheme was shown in [27] for the elastic obstacle scattering problem in three dimensions. We refer to [24] for a comprehensive account of the singular integral equations.

In this work, by using the Helmholtz decomposition, the exterior boundary value problem of the elastic obstacle scattering is reduced to a coupled boundary integral equation with the Cauchy type singular integral operators. Based on the recent works [8, 9, 20], we introduce an appropriate regularizer to the boundary integral system and split the singular integral operator in the form of an isomorphic operator plus a compact one, which enables us to derive the convergence result in some Sobolev spaces. The semi-discrete and full-discrete schemes are examined for the boundary integral system under the framework of trigonometric collocation method. We deduce the error estimates for both the semi- and full-discrete schemes and show that the numerical solution of the integral system converges to the exact solution. In particular, we demonstrate that the proposed scheme converges exponentially fast when the boundary of the obstacle and the incident wave are analytic. Numerical experiments for both smooth and nonsmooth obstacles are provided to confirm our theoretical analysis. We point out that the proposed method is able to achieve a very high precision even for boundaries with corners by using the graded meshes [4, 7, 15]. It is also worth mentioning that our method is extremely fast since the full-discrete scheme is established via simple quadrature operators. Most importantly, we only need to solve the scalar Helmholtz equation instead of solving the vector Navier equation. This feature makes the approach particularly attractive as anyone, who has the code available to solve the acoustic obstacle scattering problem, is able to adapt to solve the elastic obstacle scattering problem. The application of this formulation to elastic multi-particle scattering with fast multipole method and inverse elastic obstacle problem have been thoroughly investigated in [8, 20].

This paper concerns both the theoretical analysis and numerical computation for the elastic obstacle scattering problem. The work contains three contributions:

- (1) propose a novel boundary integral formulation by introducing a regularizer to the integral system obtained by applying the Helmholtz decomposition to the Navier equation;
- (2) establish the convergence of the semi- and full-discrete schemes of the boundary integral system via the trigonometric collocation method;
- (3) demonstrate the superior numerical performance by presenting examples of smooth and nonsmooth obstacles.

The paper is organized as follows. In Section 2, we introduce the problem formulation. Section 3 presents the boundary integral equations, gives the decomposition of integral operators, and deduces an operator equation in form of an isomorphic operator plus a compact one. Section 4 is devoted to the convergence analysis of the semi-discrete and full-discrete schemes for the boundary integral system via the trigonometric collocation method. Numerical experiments are presented to verify the theoretical findings in Section 5. The paper is concluded with some general remarks and discussions on the future work in Section 6.

2. PROBLEM FORMULATION

Consider a two-dimensional elastically rigid obstacle, which is described as a bounded domain $D \subset \mathbb{R}^2$ with an analytic boundary Γ_D . Denote by $\nu = (\nu_1, \nu_2)^\top$ and $\tau = (\tau_1, \tau_2)^\top$ the unit normal and tangential vectors on Γ_D , respectively, where $\tau_1 = -\nu_2, \tau_2 = \nu_1$. The exterior domain $\mathbb{R}^2 \setminus \overline{D}$ is assumed to be filled with a homogeneous and isotropic elastic medium with a unit mass density.

Let the obstacle be illuminated by a time-harmonic compressional plane wave $\mathbf{u}^{\text{inc}}(x) = d e^{i\kappa_p d \cdot x}$ or shear plane wave $\mathbf{u}^{\text{inc}}(x) = d^\perp e^{i\kappa_s d \cdot x}$, where $d = (\cos \theta, \sin \theta)^\top$ is the unit propagation direction vector, $\theta \in [0, 2\pi)$ is the incident angle, $d^\perp = (-\sin \theta, \cos \theta)^\top$ is an orthonormal vector of d , and

$$\kappa_p = \frac{\omega}{\sqrt{\lambda + 2\mu}}, \quad \kappa_s = \frac{\omega}{\sqrt{\mu}}$$

are the compressional wavenumber and the shear wavenumber, respectively.

The displacement of the total field \mathbf{u} satisfies the Navier equation

$$\mu \Delta \mathbf{u} + (\lambda + \mu) \nabla \nabla \cdot \mathbf{u} + \omega^2 \mathbf{u} = 0 \quad \text{in } \mathbb{R}^2 \setminus \overline{D},$$

where $\omega > 0$ is the angular frequency and λ, μ are the Lamé constants satisfying $\mu > 0, \lambda + \mu > 0$. Since the obstacle is assumed to be rigid, the total field \mathbf{u} satisfies the homogeneous boundary condition

$$\mathbf{u} = 0 \quad \text{on } \Gamma_D.$$

The total field \mathbf{u} consists of the incident field \mathbf{u}^{inc} and the scattered field \mathbf{v} , i.e.,

$$\mathbf{u} = \mathbf{u}^{\text{inc}} + \mathbf{v}.$$

It is easy to verify that the scattered field \mathbf{v} satisfies the boundary value problem

$$\begin{cases} \mu \Delta \mathbf{v} + (\lambda + \mu) \nabla \nabla \cdot \mathbf{v} + \omega^2 \mathbf{v} = 0 & \text{in } \mathbb{R}^2 \setminus \overline{D}, \\ \mathbf{v} = -\mathbf{u}^{\text{inc}} & \text{on } \Gamma_D. \end{cases} \quad (2.1)$$

In addition, the scattered field \mathbf{v} is required to satisfy the Kupradze–Sommerfeld radiation condition

$$\lim_{\rho \rightarrow \infty} \rho^{\frac{1}{2}} (\partial_\rho \mathbf{v}_p - i\kappa_p \mathbf{v}_p) = 0, \quad \lim_{\rho \rightarrow \infty} \rho^{\frac{1}{2}} (\partial_\rho \mathbf{v}_s - i\kappa_s \mathbf{v}_s) = 0, \quad \rho = |x|,$$

where

$$\mathbf{v}_p = -\frac{1}{\kappa_p^2} \nabla \nabla \cdot \mathbf{v}, \quad \mathbf{v}_s = \frac{1}{\kappa_s^2} \mathbf{curl} \mathbf{curl} \mathbf{v},$$

are known as the compressional and shear wave components of \mathbf{v} , respectively. Given a vector function $\mathbf{v} = (v_1, v_2)^\top$ and a scalar function v , the scalar and vector curl operators are defined by

$$\mathbf{curl} \mathbf{v} = \partial_{x_1} v_2 - \partial_{x_2} v_1, \quad \mathbf{curl} v = (\partial_{x_2} v, -\partial_{x_1} v)^\top.$$

For any solution \mathbf{v} of the elastic wave equation (2.1), the Helmholtz decomposition reads

$$\mathbf{v} = \nabla\phi + \mathbf{curl}\psi, \quad (2.2)$$

where ϕ, ψ are two scalar functions. Combining (2.1) and (2.2) yields the Helmholtz equations

$$\Delta\phi + \kappa_p^2\phi = 0, \quad \Delta\psi + \kappa_s^2\psi = 0.$$

As usual, ϕ and ψ are required to satisfy the Sommerfeld radiation conditions

$$\lim_{\rho \rightarrow \infty} \rho^{\frac{1}{2}}(\partial_\rho\phi - i\kappa_p\phi) = 0, \quad \lim_{\rho \rightarrow \infty} \rho^{\frac{1}{2}}(\partial_\rho\psi - i\kappa_s\psi) = 0, \quad \rho = |x|.$$

It follows from the Helmholtz decomposition and the boundary condition on Γ_D that

$$\mathbf{v} = \nabla\phi + \mathbf{curl}\psi = -\mathbf{u}^{\text{inc}}.$$

Taking the dot product of the above equation with τ and ν , respectively, we get

$$\partial_\nu\phi + \partial_\tau\psi = f_1, \quad \partial_\tau\phi - \partial_\nu\psi = f_2,$$

where

$$f_1 = -\nu \cdot \mathbf{u}^{\text{inc}}, \quad f_2 = -\tau \cdot \mathbf{u}^{\text{inc}}.$$

In summary, the scalar potential functions ϕ, ψ satisfy the coupled boundary value problem

$$\begin{cases} \Delta\phi + \kappa_p^2\phi = 0, & \Delta\psi + \kappa_s^2\psi = 0, & \text{in } \mathbb{R}^2 \setminus \overline{D}, \\ \partial_\nu\phi + \partial_\tau\psi = f_1, & \partial_\tau\phi - \partial_\nu\psi = f_2, & \text{on } \Gamma_D, \\ \lim_{\rho \rightarrow \infty} \rho^{\frac{1}{2}}(\partial_\rho\phi - i\kappa_p\phi) = 0, & \lim_{\rho \rightarrow \infty} \rho^{\frac{1}{2}}(\partial_\rho\psi - i\kappa_s\psi) = 0, & \rho = |x|. \end{cases} \quad (2.3)$$

It is well known that a radiating solution of (2.1) has the asymptotic behavior of the form

$$\mathbf{v}(x) = \frac{e^{i\kappa_p|x|}}{\sqrt{|x|}} \mathbf{v}_p^\infty(\hat{x}) + \frac{e^{i\kappa_s|x|}}{\sqrt{|x|}} \mathbf{v}_s^\infty(\hat{x}) + \mathcal{O}\left(\frac{1}{|x|^{\frac{3}{2}}}\right), \quad |x| \rightarrow \infty \quad (2.4)$$

uniformly in all directions $\hat{x} := x/|x|$, where \mathbf{v}_p^∞ and \mathbf{v}_s^∞ , defined on the unit circle Ω , are known as the compressional and shear far-field patterns of \mathbf{v} , respectively. The following result presents the relationship between the compressional (or shear) far-field pattern of \mathbf{v} and far-field patterns of ϕ (or ψ). The proof may be found in [8].

Lemma 2.1. *The far-field pattern (2.4) for the radiating solution \mathbf{v} to the Navier equation satisfies*

$$\mathbf{v}_p^\infty(\hat{x}) = i\kappa_p\phi_\infty(\hat{x})\hat{x}, \quad \mathbf{v}_s^\infty(\hat{x}) = -i\kappa_s\psi_\infty(\hat{x})\hat{x}^\perp, \quad (2.5)$$

where the complex-valued functions $\phi_\infty(\hat{x})$ and $\psi_\infty(\hat{x})$ are the far-field patterns corresponding to ϕ and ψ , respectively.

By Lemma 2.1 and the Helmholtz decomposition, it is clear that the elastic scattered field $\mathbf{v}_p, \mathbf{v}_s$ and the corresponding far-field patterns $\mathbf{v}_p^\infty, \mathbf{v}_s^\infty$ can be obtained by solving the coupled boundary value problem (2.3).

3. BOUNDARY INTEGRAL EQUATIONS

In this section, a novel boundary integral formulation is proposed for the coupled boundary value problem (2.3). In particular, a regularizer is constructed in order to handle the degenerated integral operators.

3.1. Coupled integral equations. Denote the fundamental solution to the Helmholtz equation in two dimensions by

$$\Phi(x, y; \kappa) = \frac{i}{4} H_0^{(1)}(\kappa|x - y|), \quad x \neq y,$$

where $H_0^{(1)}$ is the Hankel function of the first kind with order zero. We assume that the solution of (2.3) is given as the following single-layer potentials with densities g_1, g_2 :

$$\phi(x) = \int_{\Gamma_D} \Phi(x, y; \kappa_{\mathbf{p}}) g_1(y) ds(y), \quad \psi(x) = \int_{\Gamma_D} \Phi(x, y; \kappa_{\mathbf{s}}) g_2(y) ds(y), \quad x \in \mathbb{R}^2 \setminus \Gamma_D. \quad (3.1)$$

Letting $x \in \mathbb{R}^2 \setminus \overline{D}$ approach the boundary Γ_D in (3.1), and using the jump relation of single-layer potentials and the boundary condition of (2.3), we deduce for $x \in \Gamma_D$ that

$$\begin{aligned} -\frac{1}{2}g_1(x) + \int_{\Gamma_D} \frac{\partial \Phi(x, y; \kappa_{\mathbf{p}})}{\partial \nu(x)} g_1(y) ds(y) + \int_{\Gamma_D} \frac{\partial \Phi(x, y; \kappa_{\mathbf{s}})}{\partial \tau(x)} g_2(y) ds(y) &= -\nu(x) \cdot \mathbf{u}^{\text{inc}}(x), \\ \int_{\Gamma_D} \frac{\partial \Phi(x, y; \kappa_{\mathbf{p}})}{\partial \tau(x)} g_1(y) ds(y) + \frac{1}{2}g_2(x) - \int_{\Gamma_D} \frac{\partial \Phi(x, y; \kappa_{\mathbf{s}})}{\partial \nu(x)} g_2(y) ds(y) &= -\tau(x) \cdot \mathbf{u}^{\text{inc}}(x). \end{aligned} \quad (3.2)$$

The corresponding far-field patterns can be represented by

$$\phi_{\infty}(\hat{x}) = \gamma_{\mathbf{p}} \int_{\Gamma_D} e^{-i\kappa_{\mathbf{p}}\hat{x}\cdot y} g_1(y) ds(y), \quad \psi_{\infty}(\hat{x}) = \gamma_{\mathbf{s}} \int_{\Gamma_D} e^{-i\kappa_{\mathbf{s}}\hat{x}\cdot y} g_2(y) ds(y), \quad \hat{x} \in \Omega, \quad (3.3)$$

where $\gamma_{\sigma} = e^{i\pi/4}/\sqrt{8\kappa_{\sigma}\pi}$ for $\sigma = \mathbf{p}$ or \mathbf{s} .

We introduce the single-layer integral operator and the corresponding far-field integral operator expressed by

$$(S^{\sigma}g)(x) = 2 \int_{\Gamma_D} \Phi(x, y; \kappa_{\sigma}) g(y) ds(y), \quad (S_{\infty}^{\sigma}g)(\hat{x}) = \gamma_{\sigma} \int_{\Gamma_D} e^{-i\kappa_{\sigma}\hat{x}\cdot y} g(y) ds(y), \quad x \in \Gamma_D, \hat{x} \in \Omega.$$

In addition, we introduce the normal derivative and the tangential derivative boundary integral operators

$$(K^{\sigma}g)(x) = 2 \int_{\Gamma_D} \frac{\partial \Phi(x, y; \kappa_{\sigma})}{\partial \nu(x)} g(y) ds(y), \quad (H^{\sigma}g)(x) = 2 \int_{\Gamma_D} \frac{\partial \Phi(x, y; \kappa_{\sigma})}{\partial \tau(x)} g(y) ds(y), \quad x \in \Gamma_D.$$

Note that the operators K^{σ} and H^{σ} are defined in the sense of Cauchy principal value. Based on the boundary integral operators, the coupled boundary integral equations (3.2) can be written into the operator form

$$\begin{cases} -g_1 + K^{\mathbf{p}}g_1 + H^{\mathbf{s}}g_2 = 2f_1, \\ g_2 + H^{\mathbf{p}}g_1 - K^{\mathbf{s}}g_2 = 2f_2. \end{cases} \quad (3.4)$$

Once the system (3.4) is solved for the densities g_1 and g_2 , the corresponding far-field patterns of (3.3) can be represented as follows

$$\phi_{\infty}(\hat{x}) = (S_{\infty}^{\mathbf{p}}g_1)(\hat{x}), \quad \psi_{\infty}(\hat{x}) = (S_{\infty}^{\mathbf{s}}g_2)(\hat{x}), \quad \hat{x} \in \Omega. \quad (3.5)$$

By [20, Theorems 4.1 and 4.8], the coupled system (3.4) is uniquely solvable if neither $\kappa_{\mathbf{p}}$ nor $\kappa_{\mathbf{s}}$ is the eigenvalue of the interior Dirichlet problem for the Helmholtz equation in D . Throughout, we assume that this condition is satisfied so that the system (3.4) admits a unique solution.

3.2. Decomposition of the operators. We assume that the boundary Γ_D is an analytic curve with the parametric form

$$\Gamma_D = \{z(t) = (z_1(t), z_2(t)) : 0 \leq t < 2\pi\},$$

where $z : \mathbb{R} \rightarrow \mathbb{R}^2$ is analytic and 2π -periodic with $|z'(t)| > 0$ for all t . The parameterized integral operators are still denoted by S^σ , S_∞^σ , K^σ , and H^σ for convenience, i.e.,

$$\begin{aligned} (S^\sigma \varphi)(t) &= \frac{i}{2} \int_0^{2\pi} H_0^{(1)}(\kappa_\sigma |z(t) - z(\varsigma)|) \varphi(\varsigma) \, d\varsigma, & (K^\sigma \varphi)(t) &= \int_0^{2\pi} k^\sigma(t, \varsigma) \varphi(\varsigma) \, d\varsigma, \\ (S_\infty^\sigma \varphi)(t) &= \gamma_\sigma \int_0^{2\pi} e^{-i\kappa_\sigma \hat{x}(t) \cdot z(\varsigma)} \varphi(\varsigma) \, d\varsigma, & (H^\sigma \varphi)(t) &= \int_0^{2\pi} h^\sigma(t, \varsigma) \varphi(\varsigma) \, d\varsigma, \end{aligned}$$

where

$$\begin{aligned} k^\sigma(t, \varsigma) &= \frac{i\kappa_\sigma}{2} \mathbf{n}(t) \cdot [z(\varsigma) - z(t)] \frac{H_1^{(1)}(\kappa_\sigma |z(t) - z(\varsigma)|)}{|z(t) - z(\varsigma)|}, \\ h^\sigma(t, \varsigma) &= \frac{i\kappa_\sigma}{2} \mathbf{n}^\perp(t) \cdot [z(\varsigma) - z(t)] \frac{H_1^{(1)}(\kappa_\sigma |z(t) - z(\varsigma)|)}{|z(t) - z(\varsigma)|}, \end{aligned}$$

and

$$\begin{aligned} \mathbf{n}(t) &\stackrel{\text{def}}{=} \tilde{\nu}(t) |z'(t)| = (z_2'(t), -z_1'(t))^\top, \quad \tilde{\nu} = \nu \circ z, \\ \mathbf{n}^\perp(t) &\stackrel{\text{def}}{=} \tilde{s}(t) |z'(t)| = (z_1'(t), z_2'(t))^\top, \quad \tilde{s} = \tau \circ z. \end{aligned}$$

Multiplying $|z'|$ on both sides of (3.4), we obtain the parametric form

$$\mathcal{A}\varphi \stackrel{\text{def}}{=} \begin{bmatrix} -I + K^p & H^s \\ H^p & I - K^s \end{bmatrix} \begin{bmatrix} \varphi_1 \\ \varphi_2 \end{bmatrix} = \begin{bmatrix} w_1 \\ w_2 \end{bmatrix}, \quad (3.6)$$

where $w_j = 2(f_j \circ z)|z'|$, $\varphi_j = (g_j \circ z)|z'|$, $j = 1, 2$, and I is the identity operator.

The kernel $k^\sigma(t, \varsigma)$ of the parameterized normal derivative integral operator can be written as

$$k^\sigma(t, \varsigma) = k_1^\sigma(t, \varsigma) \ln \left(4 \sin^2 \frac{t - \varsigma}{2} \right) + k_2^\sigma(t, \varsigma),$$

where

$$\begin{aligned} k_1^\sigma(t, \varsigma) &= \frac{\kappa_\sigma}{2\pi} \mathbf{n}(t) \cdot [z(t) - z(\varsigma)] \frac{J_1(\kappa_\sigma |z(t) - z(\varsigma)|)}{|z(t) - z(\varsigma)|}, \\ k_2^\sigma(t, \varsigma) &= k^\sigma(t, \varsigma) - k_1^\sigma(t, \varsigma) \ln \left(4 \sin^2 \frac{t - \varsigma}{2} \right) \end{aligned}$$

are analytic with diagonal entries given by

$$k_1^\sigma(t, t) = 0, \quad k_2^\sigma(t, t) = \frac{1}{2\pi} \frac{\mathbf{n}(t) \cdot z''(t)}{|z'(t)|^2}.$$

Hence, $K^\sigma \varphi$ can be equivalently rewritten as

$$(K^\sigma \varphi)(t) = (K_1^\sigma \varphi)(t) + (K_2^\sigma \varphi)(t) \stackrel{\text{def}}{=} \int_0^{2\pi} \ln \left(4 \sin^2 \frac{t - \varsigma}{2} \right) k_1^\sigma(t, \varsigma) \varphi(\varsigma) \, d\varsigma + \int_0^{2\pi} k_2^\sigma(t, \varsigma) \varphi(\varsigma) \, d\varsigma.$$

Following [8], we split the kernel $h^\sigma(t, \varsigma)$ of the parameterized tangential derivative integral operator into

$$h^\sigma(t, \varsigma) = h_1(t, \varsigma) \cot \frac{\varsigma - t}{2} + h_2^\sigma(t, \varsigma) \ln \left(4 \sin^2 \frac{t - \varsigma}{2} \right) + h_3^\sigma(t, \varsigma), \quad (3.7)$$

where

$$\begin{aligned} h_1(t, \varsigma) &= \frac{1}{\pi} n^\perp(t) \cdot [z(\varsigma) - z(t)] \frac{\tan \frac{\varsigma-t}{2}}{|z(t) - z(\varsigma)|^2}, \\ h_2^\sigma(t, \varsigma) &= \frac{\kappa_\sigma}{2\pi} n^\perp(t) \cdot [z(t) - z(\varsigma)] \frac{J_1(\kappa_\sigma |z(t) - z(\varsigma)|)}{|z(t) - z(\varsigma)|}, \\ h_3^\sigma(t, \varsigma) &= h^\sigma(t, \varsigma) - h_1^\sigma(t, \varsigma) \cot \frac{\varsigma-t}{2} - h_2^\sigma(t, \varsigma) \ln \left(4 \sin^2 \frac{t-\varsigma}{2} \right) \end{aligned}$$

are analytic with diagonal entries given by

$$h_1(t, t) = \frac{1}{2\pi}, \quad h_2^\sigma(t, t) = 0, \quad h_3^\sigma(t, t) = 0.$$

In order to show the convergence, based on (3.7), we split the singular integral operator H^σ into

$$H^\sigma = H_1 + E^\sigma H_2 + \tilde{H}_1 + \tilde{H}_2^\sigma + \tilde{H}_3^\sigma, \quad (3.8)$$

where $E^\sigma \psi = \kappa_\sigma^2 |z'|^2 \psi$, and

$$\begin{aligned} (H_1 \psi)(t) &= \frac{1}{2\pi} \int_0^{2\pi} \cot \frac{\varsigma-t}{2} \psi(\varsigma) \, d\varsigma + \frac{i}{2\pi} \int_0^{2\pi} \psi(\varsigma) \, d\varsigma, \\ (H_2 \psi)(t) &= \frac{1}{4\pi} \int_0^{2\pi} \ln \left(4 \sin^2 \frac{t-\varsigma}{2} \right) \sin(t-\varsigma) \psi(\varsigma) \, d\varsigma + \frac{i}{2\pi} \int_0^{2\pi} \psi(\varsigma) \, d\varsigma, \\ (\tilde{H}_1 \psi)(t) &= \int_0^{2\pi} \tilde{h}_1(t, \varsigma) \psi(\varsigma) \, d\varsigma, \quad (\tilde{H}_2^\sigma \psi)(t) = \int_0^{2\pi} \ln \left(4 \sin^2 \frac{t-\varsigma}{2} \right) \tilde{h}_2^\sigma(t, \varsigma) \psi(\varsigma) \, d\varsigma, \\ (\tilde{H}_3^\sigma \psi)(t) &= \int_0^{2\pi} \tilde{h}_3^\sigma(t, \varsigma) \psi(\varsigma) \, d\varsigma. \end{aligned}$$

Here, the functions

$$\begin{aligned} \tilde{h}_1(t, \varsigma) &= \cot \frac{\varsigma-t}{2} \left(h_1(t, \varsigma) - \frac{1}{2\pi} \right), \\ \tilde{h}_2^\sigma(t, \varsigma) &= h_2^\sigma(t, \varsigma) - \kappa_\sigma^2 / (4\pi) |z'(t)|^2 \sin(t-\varsigma), \\ \tilde{h}_3^\sigma(t, \varsigma) &= h_3^\sigma(t, \varsigma) - i \frac{\kappa_\sigma^2 |z'(t)|^2 + 1}{2\pi} \end{aligned}$$

are analytic with diagonal entries $\tilde{h}_1(t, t) = \tilde{h}_2^\sigma(t, t) = 0$. We refer to the proof of Theorem 3.3 for the analyticity of \tilde{h}_1 .

3.3. Operator equations. We reformulate the parametrized integral equations (3.6) into a single operator form

$$\mathcal{A}\varphi = (\mathcal{H} + \mathcal{B})\varphi = w, \quad (3.9)$$

where $\varphi = (\varphi_1, \varphi_2)^\top$, $w = (w_1, w_2)^\top$ and

$$\begin{aligned} \mathcal{H} &= \begin{bmatrix} -I & H_1 \\ H_1 & I \end{bmatrix} + \begin{bmatrix} 0 & E^s H_2 \\ E^p H_2 & 0 \end{bmatrix} \stackrel{\text{def}}{=} \mathcal{H}_1 + \mathcal{H}_2, \\ \mathcal{B} &= \mathcal{B}_1 + \mathcal{B}_2 + \mathcal{B}_3 \stackrel{\text{def}}{=} \begin{bmatrix} K_1^p & \tilde{H}_2^s \\ \tilde{H}_2^p & -K_1^s \end{bmatrix} + \begin{bmatrix} K_2^p & \tilde{H}_3^s \\ \tilde{H}_3^p & -K_2^s \end{bmatrix} + \begin{bmatrix} 0 & \tilde{H}_1 \\ \tilde{H}_1 & 0 \end{bmatrix}. \end{aligned}$$

More specifically, we have

$$\begin{aligned} (\mathcal{B}_1\varphi)(t) &= \int_0^{2\pi} \ln\left(4\sin^2\frac{t-\varsigma}{2}\right) \begin{bmatrix} k_1^{\mathfrak{p}}(t, \varsigma) & \tilde{h}_2^{\mathfrak{s}}(t, \varsigma) \\ \tilde{h}_2^{\mathfrak{p}}(t, \varsigma) & -k_1^{\mathfrak{s}}(t, \varsigma) \end{bmatrix} \begin{bmatrix} \varphi_1(\varsigma) \\ \varphi_2(\varsigma) \end{bmatrix} d\varsigma, \\ (\mathcal{B}_2\varphi + \mathcal{B}_3\varphi)(t) &= \int_0^{2\pi} \begin{bmatrix} k_2^{\mathfrak{p}}(t, \varsigma) & \tilde{h}_3^{\mathfrak{s}}(t, \varsigma) + \tilde{h}_1(t, \varsigma) \\ \tilde{h}_3^{\mathfrak{p}}(t, \varsigma) + \tilde{h}_1(t, \varsigma) & -k_2^{\mathfrak{s}}(t, \varsigma) \end{bmatrix} \begin{bmatrix} \varphi_1(\varsigma) \\ \varphi_2(\varsigma) \end{bmatrix} d\varsigma. \end{aligned}$$

Let $H^p[0, 2\pi]$, $p \geq 0$ denote the space of 2π -periodic functions $u : \mathbb{R} \rightarrow \mathbb{C}$ equipped with the norm

$$\|u\|_p^2 := \sum_{m=-\infty}^{\infty} (1+m^2)^p |\hat{u}_m|^2 < \infty,$$

where

$$\hat{u}_m = \frac{1}{2\pi} \int_0^{2\pi} u(t) e^{-imt} dt, \quad m = 0, \pm 1, \pm 2, \dots$$

are the Fourier coefficients of u . Define Sobolev spaces

$$\begin{aligned} H^p[0, 2\pi]^2 &= \left\{ w = (w_1, w_2)^\top; w_1(t) \in H^p[0, 2\pi], w_2(t) \in H^p[0, 2\pi] \right\}, \\ H_*^p[0, 2\pi]^2 &= \left\{ w = (w_1, w_2)^\top; w(t) \in H^p[0, 2\pi]^2, (\mathcal{H}_1 w)(t) \in H^{p+2}[0, 2\pi]^2 \right\}, \end{aligned}$$

which are equipped with the norms

$$\begin{aligned} \|w\|_p &= \|w_1\|_p + \|w_2\|_p, \\ \|w\|_{p,*} &= \|w_1\|_p + \|w_2\|_p + \|H_1 w_2 - w_1\|_{p+2} + \|H_1 w_1 + w_2\|_{p+2}. \end{aligned} \tag{3.10}$$

It is easy to see the embedding relation $H^{p+2}[0, 2\pi]^2 \hookrightarrow H_*^p[0, 2\pi]^2 \hookrightarrow H^p[0, 2\pi]^2$ since $H_1 : H^p[0, 2\pi] \rightarrow H^p[0, 2\pi]$ is bounded (cf. Theorem 3.2).

It is difficult to analyze directly the operator equation (3.9) since the leading term \mathcal{H}_1 is degenerated [20]. To overcome this difficulty, we introduce a regularizer via multiplying both sides of (3.9) by the operator \mathcal{A} . Now, we consider the regularized equation

$$\mathcal{A}^2\varphi = (\mathcal{H}^2 + \mathcal{H}\mathcal{B} + \mathcal{B}\mathcal{H} + \mathcal{B}^2)\varphi = \mathcal{A}w, \tag{3.11}$$

which is equivalent to (3.9) since \mathcal{A} is invertible.

Theorem 3.1. *The operator $E^\sigma : H^p[0, 2\pi] \rightarrow H^p[0, 2\pi]$ is bounded.*

Proof. Recalling $E^\sigma\varphi = \kappa_\sigma^2 a(t)\varphi$ for $\sigma = \mathfrak{p}, \mathfrak{s}$, where $a(t) = |z'(t)|^2$ and is analytic, we may assume

$$a(t) = \sum_{m=-\infty}^{\infty} \hat{a}_m e^{imt},$$

where \hat{a}_m are the Fourier coefficients of a . The analyticity of a implies that

$$\sup_{m \in \mathbb{Z}} |m|^l |\hat{a}_m| < \infty \quad \forall l \geq 0,$$

which, together with [18, Corollary 8.8], gives

$$\|E^\sigma\varphi\|_p \leq c_1 \sum_{m=-\infty}^{\infty} |\hat{a}_m| |m|^k \|\varphi\|_p \leq c_1 \sum_{m=-\infty}^{\infty} |\hat{a}_m| \frac{(1+m^2)^{k/2+1}}{1+m^2} \|\varphi\|_p \leq c_2 \|\varphi\|_p,$$

where the first inequality holds for all $k \geq p$. □

Theorem 3.2. *The operator $\mathcal{H} : H^p[0, 2\pi]^2 \rightarrow H_*^p[0, 2\pi]^2$ is bounded.*

Proof. For the trigonometric basis functions $f_m(t) := e^{imt}$, $\forall m \in \mathbb{Z}$, noting

$$\begin{aligned} H_1 f_m &= \zeta_m f_m, & \zeta_m &= \begin{cases} i \operatorname{sign}(m), & m \neq 0, \\ i, & m = 0, \end{cases} \\ H_2 f_m &= \xi_m f_m, & \xi_m &= \begin{cases} \frac{i}{4} \left(\frac{1}{|m-1|} - \frac{1}{|m+1|} \right), & m = \pm 2, \pm 3, \dots, \\ -\frac{i}{8} \operatorname{sign}(m), & m = \pm 1, \\ i, & m = 0, \end{cases} \end{aligned}$$

we observe that the integral operators $H_1 : H^p[0, 2\pi] \rightarrow H^p[0, 2\pi]$ and $H_2 : H^p[0, 2\pi] \rightarrow H^{p+2}[0, 2\pi]$ are bounded for arbitrary $p \geq 0$. Then, $\forall \varphi = (\varphi_1, \varphi_2)^\top \in H^p[0, 2\pi]^2$, using $H_1 H_1 + I = 0$ and (3.10), we have

$$\begin{aligned} \|\mathcal{H}_1 \varphi\|_{p,*} &= \|(H_1 \varphi_2 - \varphi_1, H_1 \varphi_1 + \varphi_2)^\top\|_{p,*} \\ &= \|H_1 \varphi_2 - \varphi_1\|_p + \|H_1(H_1 \varphi_1 + \varphi_2) - (H_1 \varphi_2 - \varphi_1)\|_{p+2} \\ &\quad + \|H_1 \varphi_1 + \varphi_2\|_p + \|H_1(H_1 \varphi_2 - \varphi_1) + H_1 \varphi_1 + \varphi_2\|_{p+2} \\ &= \|H_1 \varphi_2 - \varphi_1\|_p + \|H_1 \varphi_1 + \varphi_2\|_p \leq C_1 \|\varphi\|_p. \end{aligned}$$

By Theorem 3.1, we get

$$\begin{aligned} \|\mathcal{H}_2 \varphi\|_{p,*} &\leq C_2 \|\mathcal{H}_2 \varphi\|_{p+2} = C_2 \|E^p H_2 \varphi_1\|_{p+2} + C_2 \|E^s H_2 \varphi_2\|_{p+2} \\ &\leq C_3 (\|\varphi_1\|_p + \|\varphi_2\|_p) = C_3 \|\varphi\|_p, \end{aligned}$$

where C_1, C_2, C_3 are positive constants. Combining the above estimates shows that $\mathcal{H} = \mathcal{H}_1 + \mathcal{H}_2 : H^p[0, 2\pi]^2 \rightarrow H_*^p[0, 2\pi]^2$ is bounded. \square

Theorem 3.3. *The operator $\mathcal{B} : H^p[0, 2\pi]^2 \rightarrow H^{p+2}[0, 2\pi]^2$ is compact.*

Proof. First we show that \mathcal{B}_1 and \mathcal{B}_2 are compact. Noting

$$k_1^\sigma(t, t) = \partial_t k_1^\sigma(t, t) = 0, \quad \tilde{h}_2^\sigma(t, t) = \partial_t \tilde{h}_2^\sigma(t, t) = 0, \quad \sigma = \mathbf{p}, \mathbf{s}, \quad (3.12)$$

and using [18, Theorems 12.15, 13.20], we get that $K_1^\sigma, H_2^\sigma : H^p[0, 2\pi] \rightarrow H^{p+3}[0, 2\pi]$ are bounded for arbitrary $p \geq 0$. Thus $\mathcal{B}_1 : H^p[0, 2\pi]^2 \rightarrow H^{p+3}[0, 2\pi]^2$ is bounded and consequently is compact from $H^p[0, 2\pi]^2$ into $H^{p+2}[0, 2\pi]^2$. Since the kernel functions k_2 and \tilde{h}_3 are analytic, it follows from [13, Theorem A.45] and [18, Theorem 8.13] that the operators $K_2^\sigma, \tilde{H}_3^\sigma : H^p[0, 2\pi] \rightarrow H^{p+r}[0, 2\pi]$ are bounded for all integer $r \geq 0$ and arbitrary $p \geq 0$. Then the operator $\mathcal{B}_2 : H^p[0, 2\pi]^2 \rightarrow H^{p+r}[0, 2\pi]^2$ is bounded for all integer $r \geq 0$ and arbitrary $p \geq 0$. In particular, the operator $\mathcal{B}_2 : H^p[0, 2\pi]^2 \rightarrow H^{p+3}[0, 2\pi]^2, \forall p \geq 0$ is bounded and consequently is compact from $H^p[0, 2\pi]^2$ into $H^{p+2}[0, 2\pi]^2$.

Next is to show the compactness of \mathcal{B}_3 . It suffices to show that \tilde{H}_1 has an analytic kernel \tilde{h}_1 . In fact, for ς sufficiently close to t , by using the Taylor expansions

$$\begin{aligned} \tan \frac{\varsigma - t}{2} &= \sum_{k=1}^{\infty} a_k \left(\frac{\varsigma - t}{2} \right)^{2k-1}, \quad a_k > 0, \quad a_1 = 1, \\ n^\perp(t) \cdot [z(\varsigma) - z(t)] &= z'_1(t) \sum_{k=1}^{\infty} \frac{z_1^{(k)}(t)}{k!} (\varsigma - t)^k + z'_2(t) \sum_{k=1}^{\infty} \frac{z_2^{(k)}(t)}{k!} (\varsigma - t)^k \\ &= |z'(t)|^2 (\varsigma - t) \left(1 + \sum_{k=1}^{\infty} b_k(t) (\varsigma - t)^k \right), \\ |z(t) - z(\varsigma)|^2 &= \left(\sum_{k=1}^{\infty} \frac{z_1^{(k)}(t)}{k!} (\varsigma - t)^k \right)^2 + \left(\sum_{k=1}^{\infty} \frac{z_2^{(k)}(t)}{k!} (\varsigma - t)^k \right)^2 \\ &= |z'(t)|^2 (\varsigma - t)^2 \left(1 + \sum_{k=1}^{\infty} d_k(t) (\varsigma - t)^k \right) \stackrel{\text{def}}{=} |z'(t)|^2 (\varsigma - t)^2 (1 + \Theta), \end{aligned}$$

we have

$$\begin{aligned} h_1(t, \varsigma) &= \frac{1}{\pi} n^\perp(t) \cdot [z(\varsigma) - z(t)] \frac{\tan \frac{\varsigma - t}{2}}{|z(t) - z(\varsigma)|^2} \\ &= \frac{1}{2\pi} \left(1 + \sum_{k=1}^{\infty} b_k(t) (\varsigma - t)^k \right) (1 - \Theta + \Theta^2 - \Theta^3 + \dots) \sum_{k=1}^{\infty} a_k \left(\frac{\varsigma - t}{2} \right)^{2k-2} \\ &= \frac{1}{2\pi} + \sum_{k=1}^{\infty} c_k(t) (\varsigma - t)^k. \end{aligned}$$

Moreover, it can be easily verified that

$$c_1(t) = \frac{b_1(t) - d_1(t)}{2\pi} = -\frac{z'_1(t)z''_1(t) + z'_2(t)z''_2(t)}{4\pi|z'(t)|^2} \neq 0.$$

Using the Taylor expansions for sine and cosine functions, we deduce that the kernel function has the expansion

$$\tilde{h}_1(t, \varsigma) = \cot \frac{\varsigma - t}{2} \sum_{k=1}^{\infty} c_k(t) (\varsigma - t)^k = \sum_{k=1}^{\infty} e_k(t) (\varsigma - t)^k, \quad e_1(t) = 2c_1(t),$$

which implies that \tilde{h}_1 is analytic and completes the proof. \square

By [18, Theorem 8.24], the operator $S_0 : H^p[0, 2\pi] \rightarrow H^{p+1}[0, 2\pi]$, defined by

$$(S_0\psi)(t) = \int_0^{2\pi} \ln \left(4 \sin^2 \frac{t - \varsigma}{2} \right) \psi(\varsigma) d\varsigma + \sqrt{2}i \int_0^{2\pi} \psi(\varsigma) d\varsigma \stackrel{\text{def}}{=} (\tilde{S}_0\psi)(t) + M_0,$$

is bounded and has a bounded inverse for all $p \geq 0$. We denote the operator \mathcal{S}_0 and \mathcal{E} by

$$\mathcal{S}_0 = \begin{bmatrix} S_0 & 0 \\ 0 & S_0 \end{bmatrix}, \quad \mathcal{E} = \frac{1}{8\pi^2} \begin{bmatrix} E^p + E^s & 0 \\ 0 & E^p + E^s \end{bmatrix}.$$

Clearly, $\mathcal{S}_0\mathcal{S}_0$ is a isomorphism from $H^p[0, 2\pi]^2$ to $H^{p+2}[0, 2\pi]^2$ and \mathcal{E} is a isomorphism from $H^p[0, 2\pi]^2$ to $H^p[0, 2\pi]^2$ since $a(t)$ is analytic and $a(t) \neq 0$.

Theorem 3.4. *For any function $\varphi \in H^p[0, 2\pi]^2$, the operator $\mathcal{H}^2 : H^p[0, 2\pi]^2 \rightarrow H^{p+2}[0, 2\pi]^2$ can be expressed as*

$$\mathcal{H}^2\varphi = (\mathcal{E}\mathcal{S}_0\mathcal{S}_0 + \mathcal{J})\varphi,$$

where \mathcal{J} is a compact operator from $H^p[0, 2\pi]^2$ into $H^{p+2}[0, 2\pi]^2$.

Proof. It follows from a straightforward calculation that

$$\begin{aligned}\mathcal{H}^2 &= \begin{bmatrix} -I & H_1 + E^s H_2 \\ H_1 + E^p H_2 & I \end{bmatrix} \begin{bmatrix} -I & H_1 + E^s H_2 \\ H_1 + E^p H_2 & I \end{bmatrix} \\ &= \begin{bmatrix} H_1 E^p H_2 + E^s H_2 H_1 & 0 \\ 0 & H_1 E^s H_2 + E^p H_2 H_1 \end{bmatrix} + \mathcal{J}_1,\end{aligned}$$

where

$$\begin{aligned}\mathcal{J}_1 &= \begin{bmatrix} E^s J_1^p H_2 & 0 \\ 0 & E^p J_1^s H_2 \end{bmatrix} + \begin{bmatrix} E^s E^p H_2 H_2 & 0 \\ 0 & E^p E^s H_2 H_2 \end{bmatrix}, \\ J_1^\sigma \psi &= H_2 E^\sigma \psi - E^\sigma H_2 \psi = \frac{\kappa_\sigma^2}{4\pi} \int_0^{2\pi} \ln \left(4 \sin^2 \frac{t-\varsigma}{2} \right) \sin(t-\varsigma) \left(|z'(\varsigma)|^2 - |z'(t)|^2 \right) \psi(\varsigma) d\varsigma \\ &\quad + \frac{i\kappa_\sigma^2}{2\pi} \int_0^{2\pi} \left(|z'(\varsigma)|^2 - |z'(t)|^2 \right) \psi(\varsigma) d\varsigma,\end{aligned}$$

and \mathcal{J}_1 is bounded from $H^p[0, 2\pi]^2$ to $H^{p+4}[0, 2\pi]^2$ and consequently is compact from $H^p[0, 2\pi]^2$ into $H^{p+2}[0, 2\pi]^2$.

For the first term of \mathcal{H}^2 , we rewrite the first diagonal element by

$$H_1 E^p H_2 + E^s H_2 H_1 = E^p H_1 H_2 + E^s H_2 H_1 + J_2^p,$$

where $J_2^p \psi = H_1 E^p H_2 \psi - E^p H_1 H_2 \psi = \tilde{J}_2^p H_2 \psi$ and

$$(\tilde{J}_2^p \psi)(t) = \frac{\kappa_p^2}{2\pi} \int_0^{2\pi} \cot \frac{t-\varsigma}{2} \left(|z'(\varsigma)|^2 - |z'(t)|^2 \right) \psi(\varsigma) d\varsigma + \frac{i\kappa_p^2}{2\pi} \int_0^{2\pi} \left(|z'(\varsigma)|^2 - |z'(t)|^2 \right) \psi(\varsigma) d\varsigma.$$

The operator J_2^p is compact from $H^p[0, 2\pi]^2$ into $H^{p+2}[0, 2\pi]^2$, since the operator \tilde{J}_2^p has an analytic kernel and H_2 is bounded. In addition, for $\psi \in H^p[0, 2\pi]$, we have

$$\begin{aligned}(H_1 H_2 \psi)(t) &= \frac{1}{2\pi} \int_0^{2\pi} \cot \frac{t-\varsigma}{2} (H_2 \psi)(\varsigma) d\varsigma + \frac{i}{2\pi} \int_0^{2\pi} (H_2 \psi)(\varsigma) d\varsigma \\ &= \frac{1}{2\pi} \int_0^{2\pi} \ln \left(4 \sin^2 \frac{t-\varsigma}{2} \right) \frac{d}{d\varsigma} (H_2 \psi)(\varsigma) d\varsigma + \frac{i}{2\pi} \xi_0 \hat{\psi}_0 2\pi \\ &= \frac{1}{2\pi} \frac{1}{4\pi} \int_0^{2\pi} \ln \left(4 \sin^2 \frac{t-\varsigma}{2} \right) \left\{ \frac{d}{d\varsigma} \int_0^{2\pi} \ln \left(4 \sin^2 \frac{\varsigma-s}{2} \right) \sin(\varsigma-s) \psi(s) ds \right\} d\varsigma - \hat{\psi}_0 \\ &= \frac{1}{8\pi^2} \int_0^{2\pi} \ln \left(4 \sin^2 \frac{t-\varsigma}{2} \right) \int_0^{2\pi} \ln \left(4 \sin^2 \frac{\varsigma-s}{2} \right) \psi(s) ds d\varsigma - \hat{\psi}_0 + \frac{1}{8\pi^2} (J_3 \psi + J_4 \psi)(t) \\ &= \frac{1}{8\pi^2} (S_0 S_0 \psi)(t) + \frac{1}{8\pi^2} (J_3 \psi)(t) + \frac{1}{8\pi^2} (J_4 \psi)(t),\end{aligned}$$

where

$$\begin{aligned}(J_3 \psi)(t) &= \int_0^{2\pi} \ln \left(4 \sin^2 \frac{t-\varsigma}{2} \right) \int_0^{2\pi} \cot \frac{\varsigma-s}{2} \sin(\varsigma-s) \psi(s) ds \stackrel{\text{def}}{=} (\tilde{S}_0 \tilde{J}_3 \psi)(t), \\ (J_4 \psi)(t) &= \int_0^{2\pi} \ln \left(4 \sin^2 \frac{t-\varsigma}{2} \right) \int_0^{2\pi} \ln \left(4 \sin^2 \frac{\varsigma-s}{2} \right) (\cos(\varsigma-s) - 1) \psi(s) ds \stackrel{\text{def}}{=} (\tilde{S}_0 \tilde{J}_4 \psi)(t),\end{aligned}$$

are compact from $H^p[0, 2\pi]^2$ into $H^{p+2}[0, 2\pi]^2$, since the operator \tilde{J}_3 has an analytic kernel and the operator $\tilde{S}_0 : H^p[0, 2\pi]^2 \rightarrow H^{p+1}[0, 2\pi]^2$ and the operator $J_4 : H^p[0, 2\pi]^2 \rightarrow H^{p+3}[0, 2\pi]^2$ are bounded. Clearly it also holds that $H_2 H_1 = H_1 H_2$.

Similarly, we can analyze the second diagonal element as the first one. Therefore, we obtain the assertion of the theorem by defining the operator

$$\mathcal{J} = \mathcal{J}_1 + \mathcal{J}_2 + \mathcal{J}_3 + \mathcal{J}_4,$$

where

$$\mathcal{J}_2 = \begin{bmatrix} J_2^p & 0 \\ 0 & J_2^s \end{bmatrix}, \quad \mathcal{J}_3 = \frac{\kappa_p^2 + \kappa_s^2}{8\pi^2} |z'|^2 \begin{bmatrix} J_3 & 0 \\ 0 & J_3 \end{bmatrix}, \quad \mathcal{J}_4 = \frac{\kappa_p^2 + \kappa_s^2}{8\pi^2} |z'|^2 \begin{bmatrix} J_4 & 0 \\ 0 & J_4 \end{bmatrix}.$$

□

4. TRIGONOMETRIC COLLOCATION METHOD

Consider the following equivalent formulation of the operator equation (3.11):

$$\mathcal{S}_0 \mathcal{S}_0 \varphi + \mathcal{E}^{-1} (\mathcal{J} + \mathcal{K}) \varphi = \mathcal{E}^{-1} \mathcal{A} w, \quad (4.1)$$

where $\mathcal{K} \stackrel{\text{def}}{=} \mathcal{H}\mathcal{B} + \mathcal{B}\mathcal{H} + \mathcal{B}^2$ is a compact operator from $H^p[0, 2\pi]^2$ into $H^{p+2}[0, 2\pi]^2$ by Theorems 3.2 and 3.3. In this section, we examine the convergence of the semi- and full-discretization of (4.1) by using the trigonometric collocation method.

4.1. Semi-discretization. Let X_n be the space of trigonometric polynomials of degree less than or equal to n of the form

$$\varphi(t) = \sum_{m=0}^n \alpha_m \cos mt + \sum_{m=1}^{n-1} \beta_m \sin mt. \quad (4.2)$$

Denote by $P_n : H^p[0, 2\pi] \rightarrow X_n$ the interpolation operator, which maps 2π -periodic scalar function g into a unique trigonometric polynomial $P_n g$ at the equidistant interpolation points $\zeta_j^{(n)} := \pi j/n$, $j = 0, \dots, 2n-1$, i.e., $(P_n g)(\zeta_j^{(n)}) = g(\zeta_j^{(n)})$. Then, P_n is a bounded linear operator.

Let $X_n^2 = \{\varphi = (\varphi_1, \varphi_2)^\top : \varphi_1 \in X_n, \varphi_2 \in X_n\}$ and define the interpolation operator $\mathcal{P}_n : H^p[0, 2\pi]^2 \rightarrow X_n^2$ by

$$\mathcal{P}_n g = (P_n g_1, P_n g_2)^\top, \quad \forall g = (g_1, g_2) \in H^p[0, 2\pi]^2.$$

Clearly, X_n^2 is unisolvent with respect to the points $\{\zeta_j^{(n)}\}_{j=0}^{2n-1}$. Moreover, we have from [18, Theorem 11.8] that

$$\|\mathcal{P}_n g - g\|_q \leq \frac{C}{n^{p-q}} \|g\|_p, \quad 0 \leq q \leq p, \quad \frac{1}{2} < p \quad (4.3)$$

for all $g \in H^p[0, 2\pi]^2$ and some constant C depending on p and q .

Now we approximate the solution $\varphi = (\varphi_1, \varphi_2)^\top$ by a trigonometric polynomial $\varphi^n = (\varphi_1^n, \varphi_2^n)^\top \in X_n^2$, which is required to satisfy the projected equation

$$\mathcal{S}_0 \mathcal{S}_0 \varphi^n + \mathcal{P}_n [\mathcal{E}^{-1} (\mathcal{J} + \mathcal{K})] \varphi^n = \mathcal{P}_n (\mathcal{E}^{-1} \mathcal{A}) w, \quad (4.4)$$

where φ^n satisfies $\mathcal{P}_n (\mathcal{S}_0 \mathcal{S}_0) \varphi^n = \mathcal{S}_0 \mathcal{S}_0 \varphi^n$.

Theorem 4.1. *For sufficiently large n , the approximate equation (4.4) is uniquely solvable and the solution satisfies the error estimate*

$$\|\varphi^n - \varphi\|_p \leq L \|\mathcal{P}_n \mathcal{S}_0 \mathcal{S}_0 \varphi - \mathcal{S}_0 \mathcal{S}_0 \varphi\|_{p+2},$$

where L is a positive constant depending on $\mathcal{E}^{-1} \mathcal{J}$, $\mathcal{E}^{-1} \mathcal{K}$ and $\mathcal{S}_0 \mathcal{S}_0$.

Proof. From the proofs of Theorems 3.3 and 3.4, we know that the operators $\mathcal{J}, \mathcal{K} : H^p[0, 2\pi]^2 \rightarrow H^{p+3}[0, 2\pi]^2, \forall p \geq 0$ are bounded. With the aid of (4.3), we deduce that

$$\|\mathcal{P}_n[\mathcal{E}^{-1}(\mathcal{J} + \mathcal{K})]\varphi - \mathcal{E}^{-1}(\mathcal{J} + \mathcal{K})\varphi\|_{p+2} \leq \frac{c_1}{n}\|\mathcal{E}^{-1}(\mathcal{J} + \mathcal{K})\varphi\|_{p+3} \leq \frac{c_2}{n}\|\varphi\|_p$$

for all $p \geq 0$ and some constants c_1 and c_2 , which implies

$$\|\mathcal{P}_n[\mathcal{E}^{-1}(\mathcal{J} + \mathcal{K})] - \mathcal{E}^{-1}(\mathcal{J} + \mathcal{K})\|_{p+2} \rightarrow 0 \quad \text{as } n \rightarrow \infty.$$

The proof is completed by noting [18, Theorem 13.12]. \square

The above theorem implies that the semi-discrete collocation method given by (4.4) converges in $H^p[0, 2\pi]^2$ for each $p \geq 0$.

4.2. Full-discretization. Denote the Lagrange basis by

$$\mathfrak{L}_j(t) = \frac{1}{2n} \left\{ 1 + 2 \sum_{k=1}^{n-1} \cos k(t - \varsigma_j^{(n)}) + \cos n(t - \varsigma_j^{(n)}) \right\}, \quad j = 0, 1, \dots, 2n-1.$$

Instead of (4.4), we find an approximate solution $\tilde{\varphi}^n \in X_n^2$ given by

$$\tilde{\varphi}^n(t) = (\tilde{\varphi}_1^n(t), \tilde{\varphi}_2^n(t))^\top = \left(\sum_{j=0}^{2n-1} \tilde{\varphi}_1^n(\varsigma_j^{(n)}) \mathfrak{L}_j(t), \sum_{j=0}^{2n-1} \tilde{\varphi}_2^n(\varsigma_j^{(n)}) \mathfrak{L}_j(t) \right)^\top,$$

which is required to satisfy

$$\mathcal{S}_{0,n} \mathcal{S}_{0,n} \tilde{\varphi}^n + \mathcal{P}_n[\mathcal{E}_n^{-1}(\mathcal{J}_n + \mathcal{K}_n)] \tilde{\varphi}^n = \mathcal{P}_n(\mathcal{E}_n^{-1} \mathcal{A}_n) w, \quad (4.5)$$

where $\mathcal{A}_n = \mathcal{H}_n + \mathcal{B}_n = \sum_{j=1}^2 \mathcal{H}_{j,n} + \sum_{j=1}^3 \mathcal{B}_{j,n}$, $\mathcal{J}_n = \sum_{j=1}^4 \mathcal{J}_{j,n}$, $\mathcal{K}_n = \mathcal{H}_n \mathcal{B}_n + \mathcal{B}_n \mathcal{H}_n + \mathcal{B}_n \mathcal{B}_n$, and the quadrature operators are described by $\mathcal{S}_{0,n} = \mathcal{S}_0 \mathcal{P}_n$, $\mathcal{H}_{1,n} = \mathcal{H}_1 \mathcal{P}_n$, $\mathcal{H}_{2,n} = \mathcal{H}_2 \mathcal{P}_n$,

$$\begin{aligned} (\mathcal{B}_{1,n} \chi)(t) &= \int_0^{2\pi} \ln \left(4 \sin^2 \frac{t-\varsigma}{2} \right) \mathcal{P}_n \left\{ \begin{bmatrix} k_1^p(t, \cdot) & \tilde{h}_2^s(t, \cdot) \\ \tilde{h}_2^p(t, \cdot) & -k_1^s(t, \cdot) \end{bmatrix} \chi \right\}(\varsigma) d\varsigma, \\ (\mathcal{B}_{2,n} \chi + \mathcal{B}_{3,n} \chi)(t) &= \int_0^{2\pi} \mathcal{P}_n \left\{ \begin{bmatrix} k_2^p(t, \cdot) & \tilde{h}_3^s(t, \cdot) + \tilde{h}_1(t, \cdot) \\ \tilde{h}_3^p(t, \cdot) + \tilde{h}_1(t, \cdot) & -k_2^s(t, \cdot) \end{bmatrix} \chi \right\}(\varsigma) d\varsigma, \end{aligned}$$

and define $E_n^\sigma \psi = \kappa_\sigma^2 |z'|^2 \psi = E^\sigma \psi$, $H_{2,n} = H_2 \mathcal{P}_n$, $\tilde{\mathcal{S}}_{0,n} = \tilde{\mathcal{S}}_0 \mathcal{P}_n$,

$$\begin{aligned} \mathcal{E}_n &= \frac{1}{8\pi^2} \begin{bmatrix} E_n^p + E_n^s & 0 \\ 0 & E_n^p + E_n^s \end{bmatrix}, \\ \mathcal{J}_{1,n} &= \begin{bmatrix} E_n^s \mathcal{J}_{1,n}^p H_{2,n} & 0 \\ 0 & E_n^p \mathcal{J}_{1,n}^s H_{2,n} \end{bmatrix} + \begin{bmatrix} E_n^s E_n^p H_{2,n} H_{2,n} & 0 \\ 0 & E_n^p E_n^s H_{2,n} H_{2,n} \end{bmatrix}, \\ \mathcal{J}_{2,n} &= \begin{bmatrix} \tilde{\mathcal{J}}_{2,n}^p H_{2,n} & 0 \\ 0 & \tilde{\mathcal{J}}_{2,n}^s H_{2,n} \end{bmatrix}, \quad \mathcal{J}_{3,n} = \frac{\kappa_p^2 + \kappa_s^2}{8\pi^2} |z'|^2 \begin{bmatrix} \tilde{\mathcal{S}}_{0,n} \tilde{\mathcal{J}}_{3,n} & 0 \\ 0 & \tilde{\mathcal{S}}_{0,n} \tilde{\mathcal{J}}_{3,n} \end{bmatrix}, \\ \mathcal{J}_{4,n} &= \frac{\kappa_p^2 + \kappa_s^2}{8\pi^2} |z'|^2 \begin{bmatrix} \tilde{\mathcal{S}}_{0,n} \tilde{\mathcal{J}}_{4,n} & 0 \\ 0 & \tilde{\mathcal{S}}_{0,n} \tilde{\mathcal{J}}_{4,n} \end{bmatrix}, \end{aligned}$$

where

$$\begin{aligned}
(J_{1,n}^\sigma \psi)(t) &= \frac{\kappa_\sigma^2}{4\pi} \int_0^{2\pi} \ln \left(4 \sin^2 \frac{t-\varsigma}{2} \right) P_n \left\{ \sin(t-\cdot) \left(|z'(\cdot)|^2 - |z'(t)|^2 \right) \psi \right\} (\varsigma) d\varsigma \\
&\quad + \frac{i\kappa_\sigma^2}{2\pi} \int_0^{2\pi} P_n \left\{ \left(|z'(\cdot)|^2 - |z'(t)|^2 \right) \psi \right\} (\varsigma) d\varsigma, \\
(\tilde{J}_{2,n}^\sigma \psi)(t) &= \frac{\kappa_\sigma^2}{2\pi} \int_0^{2\pi} P_n \left\{ \left(\cot \frac{t-\cdot}{2} + i \right) \left(|z'(\cdot)|^2 - |z'(t)|^2 \right) \psi \right\} (\varsigma) d\varsigma, \\
(\tilde{J}_{3,n} \psi)(t) &= \int_0^{2\pi} P_n \left\{ \cot \frac{t-\cdot}{2} \sin(t-\cdot) \psi \right\} (\varsigma) d\varsigma, \\
(\tilde{J}_{4,n} \psi)(t) &= \int_0^{2\pi} \ln \left(4 \sin^2 \frac{t-\varsigma}{2} \right) P_n \left\{ (\cos(t-\cdot) - 1) \psi \right\} (\varsigma) d\varsigma.
\end{aligned}$$

Clearly, $\mathcal{S}_{0,n} \mathcal{S}_{0,n} \tilde{\varphi}^n = \mathcal{S}_0 \mathcal{S}_0 \tilde{\varphi}^n$, $\mathcal{H}_n \tilde{\varphi}^n = \mathcal{H} \tilde{\varphi}^n$ for $\tilde{\varphi}^n \in X_n^2$.

In the following, we show the convergence of the full-discrete collocation method (4.5). To this end, we rewrite the function $\mathcal{B}\varphi$ in form of

$$(\mathcal{B}\varphi)(t) = \int_0^{2\pi} \ln \left(4 \sin^2 \frac{t-\varsigma}{2} \right) M(t, \varsigma) \varphi(\varsigma) d\varsigma + \int_0^{2\pi} N(t, \varsigma) \varphi(\varsigma) d\varsigma,$$

where

$$M(t, \varsigma) = \begin{bmatrix} m_1(t, \varsigma) & m_2(t, \varsigma) \\ m_3(t, \varsigma) & m_4(t, \varsigma) \end{bmatrix}, \quad N(t, \varsigma) = \begin{bmatrix} n_1(t, \varsigma) & n_2(t, \varsigma) \\ n_3(t, \varsigma) & n_4(t, \varsigma) \end{bmatrix}.$$

Noting (3.12) and the analyticity of $k_j^\sigma(t, \varsigma)$, $j = 1, 2$, $\tilde{h}_2^\sigma(t, \varsigma)$, $\tilde{h}_3^\sigma(t, \varsigma)$ and the kernel of \tilde{H}_1 , we conclude that $m_j(t, t) = \partial_t m_j(t, t) = 0$, $j = 1, 2, 3, 4$ and m_j, n_j are analytic. Recall that the full discretization of \mathcal{B} is $\mathcal{B}_n = \mathcal{B}_{1,n} + \mathcal{B}_{2,n} + \mathcal{B}_{3,n}$.

Theorem 4.2. *Assume that $0 \leq q \leq p$ and $p > 1/2$. Then for the quadrature operator \mathcal{B}_n , the following estimates hold:*

$$\|\mathcal{B}_n \varphi - \mathcal{B}\varphi\|_{q+2} \leq C \frac{1}{n^{p+1-q}} \|\varphi\|_p, \quad \|\mathcal{B}_n \chi - \mathcal{B}\chi\|_{q+2} \leq \tilde{C} \frac{1}{n^{p-q}} \|\chi\|_p \quad (4.6)$$

for all trigonometric polynomials $\varphi \in X_n^2$ and all $\chi \in H^p[0, 2\pi]^2$, and some constants C, \tilde{C} depending on p and q .

Proof. For the derivative $\frac{d}{dt}(\mathcal{B}\varphi)$, it can be written in form of

$$(\mathcal{B}'\varphi)(t) \stackrel{\text{def}}{=} \frac{d}{dt}(\mathcal{B}\varphi)(t) = \int_0^{2\pi} \ln \left(4 \sin^2 \frac{t-\varsigma}{2} \right) \tilde{M}(t, \varsigma) \varphi(\varsigma) d\varsigma + \int_0^{2\pi} \tilde{N}(t, \varsigma) \varphi(\varsigma) d\varsigma,$$

where

$$\tilde{M}(t, \varsigma) = \begin{bmatrix} \partial_t m_1(t, \varsigma) & \partial_t m_2(t, \varsigma) \\ \partial_t m_3(t, \varsigma) & \partial_t m_4(t, \varsigma) \end{bmatrix}, \quad \tilde{N}(t, \varsigma) = M(t, \varsigma) \cot \frac{t-\varsigma}{2} + \begin{bmatrix} \partial_t n_1(t, \varsigma) & \partial_t n_2(t, \varsigma) \\ \partial_t n_3(t, \varsigma) & \partial_t n_4(t, \varsigma) \end{bmatrix}.$$

We denote the full discretization of \mathcal{B}' via interpolatory quadrature by

$$(\mathcal{B}'_n \varphi)(t) = \int_0^{2\pi} \ln \left(4 \sin^2 \frac{t-\varsigma}{2} \right) \mathcal{P}_n \left\{ \tilde{M}(t, \cdot) \varphi \right\} (\varsigma) d\varsigma + \int_0^{2\pi} \mathcal{P}_n \left\{ \tilde{N}(t, \cdot) \varphi \right\} (\varsigma) d\varsigma.$$

For $p > 1/2$ and the integer q satisfying $0 \leq q \leq p$, from $\tilde{M}(t, t) = 0$ together with the analyticity of the elements in $\tilde{M}(t, \varsigma)$ and $\tilde{N}(t, \varsigma)$, using [18, Lemma 13.21 and Theorem 12.18], we have

$$\|\mathcal{B}'_n \varphi - \mathcal{B}'\varphi\|_{q+1} \leq C_1 \frac{1}{n^{p+1-q}} \|\varphi\|_p, \quad \|\mathcal{B}'_n \chi - \mathcal{B}'\chi\|_{q+1} \leq \tilde{C}_1 \frac{1}{n^{p-q}} \|\chi\|_p$$

for all trigonometric polynomials $\varphi \in X_n^2$ and some constants C_1, \tilde{C}_1 depending on p and q . Noting $\mathcal{B}'_n \varphi = \frac{d}{dt}(\mathcal{B}_n \varphi)$, the above equation implies

$$\|\mathcal{B}_n \varphi - \mathcal{B} \varphi\|_{q+2} \leq C_2 \frac{1}{n^{p+1-q}} \|\varphi\|_p, \quad \|\mathcal{B}_n \chi - \mathcal{B} \chi\|_{q+2} \leq \tilde{C}_2 \frac{1}{n^{p-q}} \|\chi\|_p$$

for some constants C_2, \tilde{C}_2 depending on p and q . It follows from [18, Theorem 8.13] that the above inequality holds for arbitrary q satisfying $0 \leq q \leq p$ and $p > 1/2$, which completes the proof. \square

In the following, the notation $a \lesssim b$ means $a \leq Cb$, where $C > 0$ is a constant depending on p .

Theorem 4.3. *Assume that $p > 1/2$. Then for the quadrature operator \mathcal{K}_n , the following estimate holds:*

$$\|\mathcal{P}_n[\mathcal{E}_n^{-1} \mathcal{K}_n - \mathcal{E}^{-1} \mathcal{K}] \varphi\|_{p+2} \lesssim \frac{1}{n} \|\varphi\|_p$$

for all trigonometric polynomials $\varphi \in X_n^2$.

Proof. From Theorem 3.2 and the estimate (4.3), $\forall \chi \in H^p[0, 2\pi]^2$, we have

$$\|(\mathcal{H}_n - \mathcal{H})\chi\|_{q,*} = \|\mathcal{H}(\mathcal{P}_n \chi - \chi)\|_{q,*} \leq C_1 \|(\mathcal{P}_n \chi - \chi)\|_q \leq \frac{C_2}{n^{p-q}} \|\chi\|_p$$

for $0 \leq q \leq p$, $p \geq 1/2$ and some constants C_1 depending on q and C_2 depending on p and q . Then, \mathcal{H}_n and $\mathcal{H}_n - \mathcal{H}$ are uniformly bounded from $H^p[0, 2\pi]^2$ to $H_*^p[0, 2\pi]^2$ for $p \geq 1/2$. Clearly, $\mathcal{E}_n^{-1} \chi = \mathcal{E}^{-1} \chi$.

For all trigonometric polynomials $\varphi \in X_n^2$ of the form (4.2), using Theorem 4.2 and the fact that $\mathcal{H}_n \varphi = \mathcal{H} \varphi$, we get

$$\begin{aligned} \|\mathcal{H}_n \mathcal{B}_n \varphi - \mathcal{H} \mathcal{B} \varphi\|_{p+2} &\leq \|\mathcal{H}_n \mathcal{B}_n \varphi - \mathcal{H} \mathcal{B} \varphi\|_{p+2,*} \\ &\leq \|\mathcal{H}_n (\mathcal{B}_n - \mathcal{B}) \varphi\|_{p+2,*} + \|(\mathcal{H}_n - \mathcal{H})(\mathcal{B} \varphi - \mathcal{P}_n \mathcal{B} \varphi)\|_{p+2,*} + \|(\mathcal{H}_n - \mathcal{H}) \mathcal{P}_n \mathcal{B} \varphi\|_{p+2,*} \\ &\lesssim \|(\mathcal{B}_n - \mathcal{B}) \varphi\|_{p+2} + \|\mathcal{B} \varphi - \mathcal{P}_n \mathcal{B} \varphi\|_{p+2} \\ &\lesssim 1/n \|\varphi\|_p + 1/n \|\mathcal{B} \varphi\|_{p+3} \lesssim 1/n \|\varphi\|_p \end{aligned}$$

Furthermore, it follows from Theorem 4.2 that \mathcal{B}_n and $\mathcal{B}_n - \mathcal{B}$ are uniformly bounded from $H^p[0, 2\pi]^2$ to $H^{p+2}[0, 2\pi]^2$ for $p \geq 1/2$. Thus, using (4.3), (4.6) and the uniform boundedness of $\mathcal{P}_n : H^{p+2}[0, 2\pi]^2 \rightarrow H^{p+2}[0, 2\pi]^2$, together with the boundedness of $\mathcal{B} : H^p[0, 2\pi]^2 \rightarrow H^{p+3}[0, 2\pi]^2$, we deduce

$$\begin{aligned} \|\mathcal{B}_n^2 \varphi - \mathcal{B}^2 \varphi\|_{p+2} &\leq \|\mathcal{B}_n^2 \varphi - \mathcal{B}^2 \varphi\|_{p+4} \\ &\leq \|\mathcal{B}_n (\mathcal{B}_n - \mathcal{B}) \varphi\|_{p+4} + \|(\mathcal{B}_n - \mathcal{B})(\mathcal{B} \varphi - \mathcal{P}_n \mathcal{B} \varphi)\|_{p+4} + \|(\mathcal{B}_n - \mathcal{B}) \mathcal{P}_n \mathcal{B} \varphi\|_{p+4} \\ &\lesssim \|(\mathcal{B}_n - \mathcal{B}) \varphi\|_{p+2} + \|(\mathcal{B} \varphi - \mathcal{P}_n \mathcal{B} \varphi)\|_{p+2} + 1/n \|\mathcal{P}_n \mathcal{B} \varphi\|_{p+2} \\ &\lesssim 1/n \|\varphi\|_p + 1/n \|\mathcal{B} \varphi\|_{p+3} + 1/n \|\mathcal{B} \varphi\|_{p+2} \lesssim 1/n \|\varphi\|_p. \end{aligned}$$

Noting $\mathcal{H}_1 \varphi \in X_n^2$, we obtain

$$\begin{aligned} \|\mathcal{B}_n \mathcal{H}_n \varphi - \mathcal{B} \mathcal{H} \varphi\|_{p+2} &= \|(\mathcal{B}_n - \mathcal{B}) \mathcal{H} \varphi\|_{p+2} \\ &\leq \|(\mathcal{B}_n - \mathcal{B})(\mathcal{H} \varphi - \mathcal{P}_n \mathcal{H} \varphi)\|_{p+2} + \|(\mathcal{B}_n - \mathcal{B}) \mathcal{P}_n \mathcal{H} \varphi\|_{p+2} \\ &\lesssim \|\mathcal{H} \varphi - \mathcal{P}_n \mathcal{H} \varphi\|_p + 1/n \|\mathcal{P}_n \mathcal{H} \varphi\|_p \\ &\leq \|\mathcal{H}_1 \varphi - \mathcal{P}_n \mathcal{H}_1 \varphi\|_p + \|\mathcal{H}_2 \varphi - \mathcal{P}_n \mathcal{H}_2 \varphi\|_p + 1/n \|\mathcal{P}_n \mathcal{H} \varphi\|_p \\ &\lesssim 1/n^2 \|\mathcal{H}_2 \varphi\|_{p+2} + 1/n \|\mathcal{H} \varphi\|_p \lesssim 1/n \|\varphi\|_p. \end{aligned}$$

Therefore

$$\|\mathcal{K}_n \varphi - \mathcal{K} \varphi\|_{p+2} \leq \|\mathcal{H}_n \mathcal{B}_n \varphi - \mathcal{H} \mathcal{B} \varphi\|_{p+2} + \|\mathcal{B}_n \mathcal{H}_n \varphi - \mathcal{B} \mathcal{H} \varphi\|_{p+2} + \|\mathcal{B}_n^2 \varphi - \mathcal{B}^2 \varphi\|_{p+2} \lesssim 1/n \|\varphi\|_p.$$

The proof is completed by using the uniform boundedness of the operator $\mathcal{E}^{-1}, \mathcal{P}_n : H^{p+2}[0, 2\pi]^2 \rightarrow H^{p+2}[0, 2\pi]^2$. \square

Theorem 4.4. *Assume that $p > 1/2$. Then for the quadrature operator \mathcal{J}_n , the following estimate holds:*

$$\|\mathcal{P}_n[\mathcal{E}_n^{-1}\mathcal{J}_n - \mathcal{E}^{-1}\mathcal{J}]\varphi\|_{p+2} \lesssim \frac{1}{n}\|\varphi\|_p$$

for all trigonometric polynomials $\varphi \in X_n^2$.

Proof. For all trigonometric polynomials $\varphi \in X_n^2$, we claim that

$$\|\mathcal{J}_n\varphi - \mathcal{J}\varphi\|_{p+2} \lesssim \frac{1}{n}\|\varphi\|_p.$$

In fact, analogous to the discussion in Theorem 4.2, we get

$$\begin{aligned} \|J_{1,n}^\sigma\psi - J_1^\sigma\psi\|_{q+2} &\leq C\frac{1}{n^{p+1-q}}\|\psi\|_p, & 0 \leq q \leq p, & \frac{1}{2} < p, \\ \|\tilde{J}_{4,n}\psi - \tilde{J}_4\psi\|_{q+2} &\leq C\frac{1}{n^{p+1-q}}\|\psi\|_p, & 0 \leq q \leq p, & \frac{1}{2} < p, \end{aligned}$$

for all trigonometric polynomials $\psi \in X_n$ and some constant C depending on p and q . Since $E_n^\sigma\varphi_j = E^\sigma\varphi_j$, $H_{2,n}\varphi_j = H_2\varphi_j \in X_n$, $j = 1, 2$, we have

$$\begin{aligned} \|\mathcal{J}_{1,n}\varphi - \mathcal{J}_1\varphi\|_{p+2} &= \|(E_n^s J_{1,n}^p H_{2,n} - E^s J_1^p H_2)\varphi_1\|_{p+2} + \|(E_n^p J_{1,n}^s H_{2,n} - E^p J_1^s H_2)\varphi_2\|_{p+2} \\ &\lesssim \|(J_{1,n}^p - J_1^p)H_2\varphi_1\|_{p+2} + \|(J_{1,n}^s - J_1^s)H_2\varphi_2\|_{p+2} \\ &\leq \|(J_{1,n}^p - J_1^p)H_2\varphi_1\|_{p+4} + \|(J_{1,n}^s - J_1^s)H_2\varphi_2\|_{p+4} \\ &\lesssim 1/n\|H_2\varphi_1\|_{p+2} + 1/n\|H_2\varphi_2\|_{p+2} \lesssim 1/n\|\varphi\|_p. \end{aligned}$$

Since the operator \tilde{J}_2^σ has an analytic kernel, it is easy to see

$$\|\mathcal{J}_{2,n}\varphi - \mathcal{J}_2\varphi\|_{p+2} \lesssim \frac{1}{n}\|\varphi\|_p.$$

In addition, in terms of $\tilde{S}_{0,n}\psi = \tilde{S}_0\psi$ for $\psi \in X_n$ and the uniform boundedness of $\tilde{S}_{0,n}$ and $\tilde{S}_{0,n} - \tilde{S}_0$ from $H^p[0, 2\pi]^2$ to $H^{p+1}[0, 2\pi]^2$ for $p \geq 1/2$, we obtain

$$\begin{aligned} \|\mathcal{J}_{4,n}\varphi - \mathcal{J}_4\varphi\|_{p+2} &= \frac{1}{8\pi^2} \sum_{j=1}^2 \left\| \left((E_n^p + E_n^s)\tilde{S}_{0,n}\tilde{J}_{4,n} - (E^p + E^s)\tilde{S}_0\tilde{J}_4 \right) \varphi_j \right\|_{p+2} \\ &\lesssim \sum_{j=1}^2 \left\| (\tilde{S}_{0,n}\tilde{J}_{4,n} - \tilde{S}_0\tilde{J}_4)\varphi_j \right\|_{p+2} \\ &\leq \sum_{j=1}^2 \left(\|\tilde{S}_{0,n}(\tilde{J}_{4,n} - \tilde{J}_4)\varphi_j\|_{p+2} + \|(\tilde{S}_{0,n} - \tilde{S}_0)(\tilde{J}_4\varphi_j - P_n\tilde{J}_4\varphi_j)\|_{p+2} \right) \\ &\leq \sum_{j=1}^2 \left(\|\tilde{S}_{0,n}(\tilde{J}_{4,n} - \tilde{J}_4)\varphi_j\|_{p+3} + \|(\tilde{S}_{0,n} - \tilde{S}_0)(\tilde{J}_4\varphi_j - P_n\tilde{J}_4\varphi_j)\|_{p+3} \right) \\ &\lesssim \sum_{j=1}^2 \left(\|(\tilde{J}_{4,n} - \tilde{J}_4)\varphi_j\|_{p+2} + \|(\tilde{J}_4\varphi_j - P_n\tilde{J}_4\varphi_j)\|_{p+2} \right) \\ &\lesssim \sum_{j=1}^2 \left(\frac{1}{n}\|\varphi_j\|_{p+2} + \frac{1}{n}\|(\tilde{J}_4\varphi_j)\|_{p+3} \right) \lesssim \frac{1}{n}\|\varphi\|_p. \end{aligned}$$

Since the operator $\tilde{\mathcal{J}}_3$ has an analytic kernel, similarly we get

$$\|\mathcal{J}_{3,n}\varphi - \mathcal{J}_3\varphi\|_{p+2} \lesssim \frac{1}{n}\|\varphi\|_p.$$

Hence, the assertion of the theorem follows by using the uniform boundedness of the operator $\mathcal{E}^{-1}, \mathcal{P}_n : H^{p+2}[0, 2\pi]^2 \rightarrow H^{p+2}[0, 2\pi]^2$. \square

Theorem 4.5. *For sufficiently large n , the approximate equation (4.5) is uniquely solvable and the solution satisfies the error estimate*

$$\begin{aligned} \|\tilde{\varphi}^n - \varphi\|_p \leq L \left\{ \|\mathcal{P}_n \mathcal{S}_0 \mathcal{S}_0 \varphi - \mathcal{S}_0 \mathcal{S}_0 \varphi\|_{p+2} + \|\mathcal{P}_n [\mathcal{E}_n^{-1}(\mathcal{J}_n + \mathcal{K}_n) - \mathcal{E}^{-1}(\mathcal{J} + \mathcal{K})]\varphi\|_{p+2} \right\} \\ + L \|\mathcal{P}_n [\mathcal{E}_n^{-1} \mathcal{A}_n - \mathcal{E}^{-1} \mathcal{A}]w\|_{p+2}, \end{aligned} \quad (4.7)$$

where L is a positive constant.

Proof. For all trigonometric polynomials $\varphi \in X_n^2$, it follows from Theorems 4.3 and 4.4 that

$$\|\mathcal{P}_n [\mathcal{E}_n^{-1}(\mathcal{J}_n + \mathcal{K}_n) - \mathcal{E}^{-1}(\mathcal{J} + \mathcal{K})]\varphi\|_{p+2} \lesssim \frac{1}{n}\|\varphi\|_p \rightarrow 0, \quad n \rightarrow \infty$$

for all $p > 1/2$. Moreover, it is easy to see the estimates for $\|(J_{1,n}^\sigma - J_1^\sigma)\psi\|_{p+2}$ and $\|(\tilde{J}_{4,n} - \tilde{J}_4)\psi\|_{p+2}$ are valid analogously as (4.6). Then, we can obtain the uniform boundedness of the operator $\mathcal{P}_n [\mathcal{E}_n^{-1}(\mathcal{J}_n + \mathcal{K}_n) - \mathcal{E}^{-1}(\mathcal{J} + \mathcal{K})] : H^p[0, 2\pi]^2 \rightarrow H^{p+2}[0, 2\pi]^2$ from the proofs of Theorems 4.3 and 4.4. By the Banach–Steinhaus theorem (cf. [18, Problem 10.1]), we get the pointwise convergence

$$\mathcal{P}_n [\mathcal{E}_n^{-1}(\mathcal{J}_n + \mathcal{K}_n)]\varphi \rightarrow \mathcal{P}_n [\mathcal{E}^{-1}(\mathcal{J} + \mathcal{K})]\varphi \quad \text{as } n \rightarrow \infty$$

for all $\varphi \in H^p[0, 2\pi]^2$.

Hence (4.7) follows by employing [18, Corollary 13.13], $\mathcal{E}_n^{-1} = \mathcal{E}^{-1}$ and the uniform boundedness of the operator $\mathcal{E}_n^{-1}, \mathcal{P}_n : H^{p+2}[0, 2\pi]^2 \rightarrow H^{p+2}[0, 2\pi]^2$. \square

The above theorem implies that the full-discrete collocation method (4.5) converges in $H^p[0, 2\pi]^2$ for each $p > 1/2$.

5. NUMERICAL EXPERIMENTS

In practice, instead of (4.5), we only need to solve the equivalent full-discrete equation

$$\mathcal{P}_n \mathcal{H}_n \tilde{\varphi}^n + \mathcal{P}_n \mathcal{B}_n \tilde{\varphi}^n = \mathcal{P}_n w \Leftrightarrow A_n \tilde{\varphi}^n = w^n, \quad (5.1)$$

where A_n is a coefficient matrix of the full-discrete equation. In fact, suppose that $\beta(t) = \frac{\kappa_p^2 + \kappa_s^2}{8\pi^2} |z'(t)|^2$, the equation (4.5) is equivalent to

$$\begin{aligned} \mathcal{P}_n (\mathcal{S}_{0,n} \mathcal{S}_{0,n}) \tilde{\varphi}^n + \mathcal{P}_n [\beta^{-1}(\mathcal{J}_n + \mathcal{K}_n)] \tilde{\varphi}^n &= \mathcal{P}_n [\beta^{-1} \mathcal{A}_n w] \\ \Leftrightarrow \mathcal{P}_n [\beta(\mathcal{S}_{0,n} \mathcal{S}_{0,n}) \tilde{\varphi}^n] + \mathcal{P}_n [(\mathcal{J}_n + \mathcal{K}_n) \tilde{\varphi}^n] &= \mathcal{P}_n (\mathcal{A}_n w) \\ \Leftrightarrow A_n^2 \tilde{\varphi}^n &= A_n w^n. \end{aligned} \quad (5.2)$$

Since (4.5) is uniquely solvable by Theorem 4.5, it implies that the matrix A_n^2 is invertible, i.e., $\det A_n^2 = (\det A_n)^2 \neq 0$, and consequently A_n is invertible. Hence, (4.5) is equivalent to (5.1) by multiplying matrix A_n^{-1} on both ends of the equation (5.2). It is worth mentioning that the equivalent full-discrete equation (5.1) is extremely efficient since it is established via simple quadrature operators \mathcal{H}_n and \mathcal{B}_n .

For the smooth integrals, we simply use the trapezoidal rule

$$\int_0^{2\pi} f(\varsigma) d\varsigma \approx \frac{\pi}{n} \sum_{j=0}^{2n-1} f(\varsigma_j^{(n)}).$$

For the singular integrals, we employ the following quadrature rules via the trigonometric interpolation:

$$\begin{aligned} \int_0^{2\pi} \ln \left(4 \sin^2 \frac{t-\varsigma}{2} \right) f(\varsigma) \, d\varsigma &\approx \sum_{j=0}^{2n-1} R_j^{(n)}(t) f(\varsigma_j^{(n)}), \\ \frac{1}{2\pi} \int_0^{2\pi} \cot \frac{\varsigma-t}{2} f(\varsigma) \, d\varsigma &\approx \sum_{j=0}^{2n-1} U_j^{(n)}(t) f(\varsigma_j^{(n)}), \\ \int_0^{2\pi} \ln \left(4 \sin^2 \frac{t-\varsigma}{2} \right) \sin(t-\varsigma) f(\varsigma) \, d\varsigma &\approx \sum_{j=0}^{2n-1} V_j^{(n)}(t) f(\varsigma_j^{(n)}), \end{aligned} \quad (5.3)$$

where the quadrature weights are given by

$$\begin{aligned} R_j^{(n)}(t) &= -\frac{2\pi}{n} \sum_{m=1}^{n-1} \frac{1}{m} \cos \left[m(t - \varsigma_j^{(n)}) \right] - \frac{\pi}{n^2} \cos \left[n(t - \varsigma_j^{(n)}) \right], \\ U_j^{(n)}(t) &= \frac{1}{2n} \left[1 - \cos n(\varsigma_j^{(n)} - t) \right] \cot \frac{\varsigma_j^{(n)} - t}{2}, \\ V_j^{(n)}(t) &= -\frac{\pi}{2n} \sin(\varsigma_j^{(n)} - t) + \frac{2\pi}{n} \sum_{m=2}^{n-1} \frac{\sin \left[m(\varsigma_j^{(n)} - t) \right]}{m^2 - 1} + \frac{2\pi \sin \left[n(\varsigma_j^{(n)} - t) \right]}{n(n^2 - 1)}. \end{aligned}$$

Here, the weight $V_j^{(n)}$ is calculated by using [18, Lemma 8.23] and we also refer to [18] for the weights $R_j^{(n)}$ and $U_j^{(n)}$. On the other hand, the last items of $\mathcal{H}_{1,n}$ and $\mathcal{H}_{2,n}$ can be offset by the following item

$$\int_0^{2\pi} \mathcal{P}_n \left\{ \begin{bmatrix} 0 & \tilde{h}_3^s(t, \cdot) - h_3^s(t, \cdot) \\ \tilde{h}_3^p(t, \cdot) - h_3^p(t, \cdot) & 0 \end{bmatrix} \chi \right\}(\varsigma) \, d\varsigma$$

in $\mathcal{B}_{2,n}$. Thus, the equation (5.1) becomes

$$\begin{aligned} w_{1,i}^{(n)} &= -\varphi_{1,i}^{(n)} + \sum_{j=0}^{2n-1} X_{ij,p}^{(n)} \varphi_{1,j}^{(n)} + \sum_{j=0}^{2n-1} Y_{ij,s}^{(n)} \varphi_{2,j}^{(n)}, \\ w_{2,i}^{(n)} &= \varphi_{2,i}^{(n)} + \sum_{j=0}^{2n-1} Y_{ij,p}^{(n)} \varphi_{1,j}^{(n)} - \sum_{j=0}^{2n-1} X_{ij,s}^{(n)} \varphi_{2,j}^{(n)}, \end{aligned} \quad (5.4)$$

where $w_{l,i}^{(n)} = w_l(\varsigma_i^{(n)})$, $\varphi_{l,i}^{(n)} = \varphi_l(\varsigma_i^{(n)})$ for $i, j = 0, \dots, 2n-1$, $l = 1, 2$, and

$$\begin{aligned} X_{ij,\sigma}^{(n)} &= R_j^{(n)}(\varsigma_i^{(n)}) k_1^\sigma(\varsigma_i^{(n)}, \varsigma_j^{(n)}) + \frac{\pi}{n} k_2^\sigma(\varsigma_i^{(n)}, \varsigma_j^{(n)}), \\ Y_{ij,\sigma}^{(n)} &= U_j^{(n)}(\varsigma_i^{(n)}) + \frac{\kappa_\sigma^2}{4\pi} |z'(\varsigma_i^{(n)})|^2 V_j^{(n)}(\varsigma_i^{(n)}) + R_j^{(n)}(\varsigma_i^{(n)}) \tilde{h}_2^\sigma(\varsigma_i^{(n)}, \varsigma_j^{(n)}) \\ &\quad + \frac{\pi}{n} h_3^\sigma(\varsigma_i^{(n)}, \varsigma_j^{(n)}) + \frac{\pi}{n} \tilde{h}_1(\varsigma_i^{(n)}, \varsigma_j^{(n)}). \end{aligned}$$

Remark 5.1. *Moreover, a straightforward calculation yields*

$$V_j^{(n)}(t) - R_j^{(n)}(t) \sin(t - \varsigma_j^{(n)}) = \frac{\pi \sin n(t - \varsigma_j^{(n)})}{n(n+1)} + \frac{\pi}{n^2} \sin n(t - \varsigma_j^{(n)}) \cos(t - \varsigma_j^{(n)}),$$

which implies $V_j^{(n)}(\varsigma_i^{(n)}) - R_j^{(n)}(\varsigma_i^{(n)}) \sin(\varsigma_i^{(n)} - \varsigma_j^{(n)}) = 0$. Therefore, $Y_{ij,\sigma}^{(n)}$ can be reduced to

$$Y_{ij,\sigma}^{(n)} = U_j^{(n)}(\varsigma_i^{(n)}) + R_j^{(n)}(\varsigma_i^{(n)}) h_2^\sigma(\varsigma_i^{(n)}, \varsigma_j^{(n)}) + \frac{\pi}{n} h_3^\sigma(\varsigma_i^{(n)}, \varsigma_j^{(n)}) + \frac{\pi}{n} \tilde{h}_1(\varsigma_i^{(n)}, \varsigma_j^{(n)}).$$

TABLE 1. Parametrization of the exact boundary curves.

Type	Parametrization
Apple-shaped	$z(t) = \frac{0.55(1 + 0.9 \cos t + 0.1 \sin 2t)}{1 + 0.75 \cos t}(\cos t, \sin t), \quad t \in [0, 2\pi]$
Peach-shaped	$z(t) = 0.22(\cos^2 t \sqrt{1 - \sin t} + 2)(\cos t, \sin t), \quad t \in [0, 2\pi]$
Drop-shaped	$z(t) = (2 \sin \frac{t}{2} - 1, -\sin t), \quad t \in [0, 2\pi]$
Heart-shaped	$z(t) = (\frac{3}{2} \sin \frac{3t}{2}, \sin t), \quad t \in [0, 2\pi]$

TABLE 2. Numerical errors for the apple-shaped and peach-shaped obstacles with $\omega = \pi$.

n	Apple-shaped		Peach-shaped	
	$\ \phi_* - \phi^{(n)}\ _{L^2}$	$\ \psi_* - \psi^{(n)}\ _{L^2}$	$\ \phi_* - \phi^{(n)}\ _{L^2}$	$\ \psi_* - \psi^{(n)}\ _{L^2}$
8	0.0677	0.0613	0.0044	0.0050
16	2.1192e-04	1.6939e-04	3.9734e-04	4.5298e-04
32	3.7880e-07	3.0432e-07	5.4337e-05	6.1341e-05
64	6.6341e-12	5.2998e-12	6.9918e-06	7.8543e-06
128	1.6200e-15	1.6162e-15	8.8584e-07	9.9062e-07
256	1.9389e-15	2.2955e-15	1.1140e-07	1.2420e-07
512	3.1540e-15	2.9617e-15	1.3962e-08	1.5539e-08
1024	4.2380e-15	3.7504e-15	1.7475e-09	1.9429e-09

TABLE 3. Numerical errors for the apple-shaped and peach-shaped obstacles with $\omega = 100\pi$.

n	Apple-shaped		Peach-shaped	
	$\ \phi_* - \phi^{(n)}\ _{L^2}$	$\ \psi_* - \psi^{(n)}\ _{L^2}$	$\ \phi_* - \phi^{(n)}\ _{L^2}$	$\ \psi_* - \psi^{(n)}\ _{L^2}$
64	2.2192	1.1012	5.9298	2.5847
128	7.2908e-02	9.2983e-02	1.0250e-01	1.0459e-01
256	5.5220e-07	1.0522e-06	4.1347e-07	9.4716e-07
512	6.0630e-13	4.4848e-13	5.0089e-08	3.6659e-08
1024	5.3276e-13	3.7980e-13	6.2029e-09	4.3889e-09
2048	4.8503e-13	4.0631e-13	7.7281e-10	5.3866e-10
4096	5.3277e-13	3.9049e-13	9.6473e-11	6.6741e-11

From this, we find that $E^\sigma H_2\varphi$ in (3.8) is only used for the theoretical analysis.

Remark 5.2. From [14, Section 4], we know that the trapezoidal rule and the quadrature formulas (5.3) yield convergence of exponential order for periodic analytic function f . In addition, from [18, Theorem 11.7], we conclude exponential convergence of our method if the boundary of obstacle and the exact solution are analytic.

5.1. Numerical examples: smooth obstacles. In this subsection, we consider the elastic scattering by an apple-shaped and a peach-shaped obstacle with analytic and C^2 boundary, respectively. The parametrizations of these two boundary curves are given in Table 1. To test the accuracy of the trigonometric collocation method, we construct an exact solution by letting the exterior field of

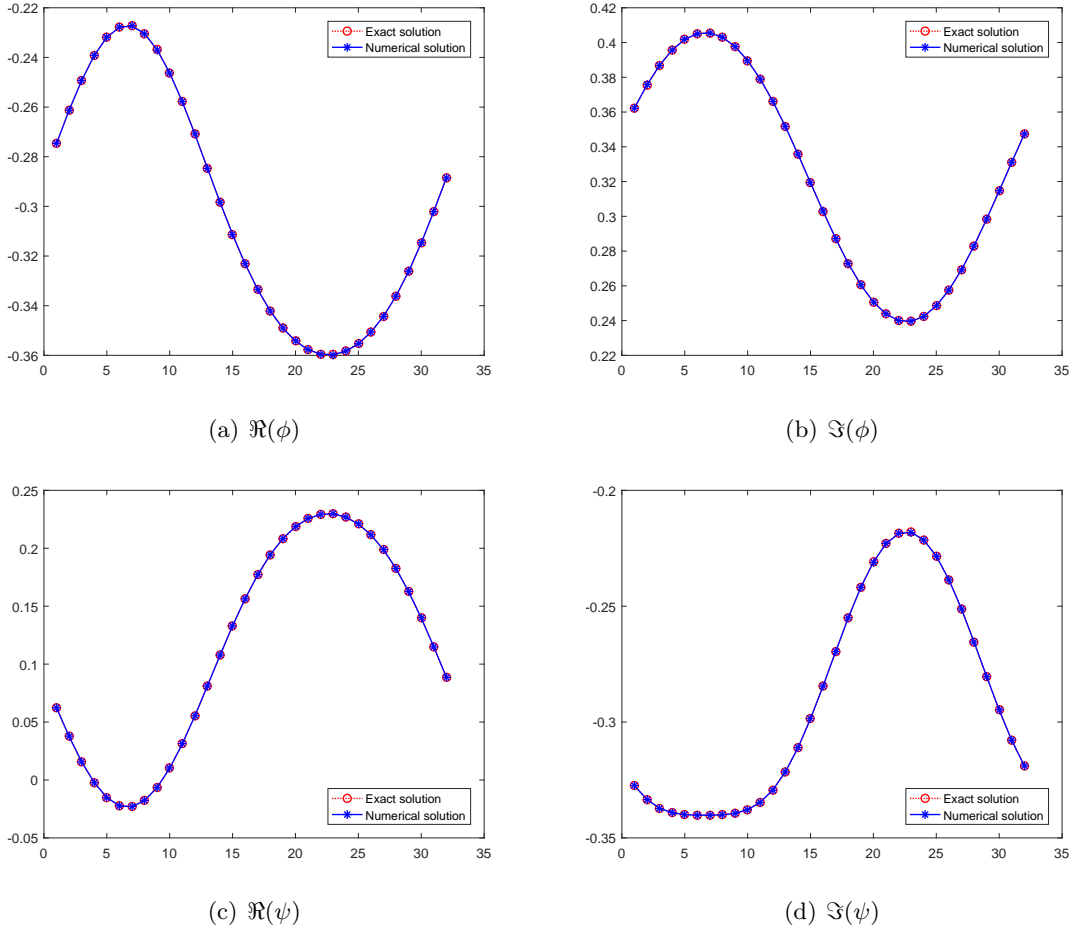


FIGURE 1. Numerical solutions and corresponding exact solutions for the apple-shaped obstacle with $\omega = \pi, n = \tilde{n} = 16$.

the elastic obstacle be generated by two point sources located at $\bar{x} = (0.1, 0.2)^\top \in D$, i.e.,

$$\phi_*(x) = H_0^{(1)}(\kappa_p |x - \bar{x}|), \quad \psi_*(x) = H_0^{(1)}(\kappa_s |x - \bar{x}|), \quad x \in \mathbb{R}^2 \setminus \bar{D}. \quad (5.5)$$

Due to the uniqueness of the boundary value problem (2.3), the solution can be constructed explicitly by enforcing the following boundary conditions on Γ_D :

$$f_1 = \partial_\nu \phi_* + \partial_\tau \psi_*, \quad f_2 = \partial_\tau \phi_* - \partial_\nu \psi_*.$$

In numerical experiments, we take the Lamé parameters $\lambda = 3.88, \mu = 2.56$ and let the observation points be generated by $\{\varsigma_i^{(n)}\}_{i=0}^{2\tilde{n}-1}$, $\tilde{n} = 16$ are distributed on a circle $\partial B = \{x \in \mathbb{R}^2 : |x| = 3\}$. We list the numerical errors between the numerical solution and the corresponding exact solution with $L^2(\partial B)$ norm in Tables 2 and 3 for the angular frequency $\omega = \pi$ and $\omega = 100\pi$, respectively. It can be easily seen from the results that the accuracy is improved dramatically as the number of collocation points are increased. In fact, our method has an exponential convergence which confirms the theoretical analysis. We also find that the convergence rate of the apple-shaped obstacle with analytic boundary is faster than that of the peach-shaped obstacle with \mathcal{C}^2 boundary. The numerical solution and the corresponding exact solution are shown in Figure 1 for the apple-shaped obstacle. Clearly they coincide perfectly with $\omega = \pi, n = 16$.

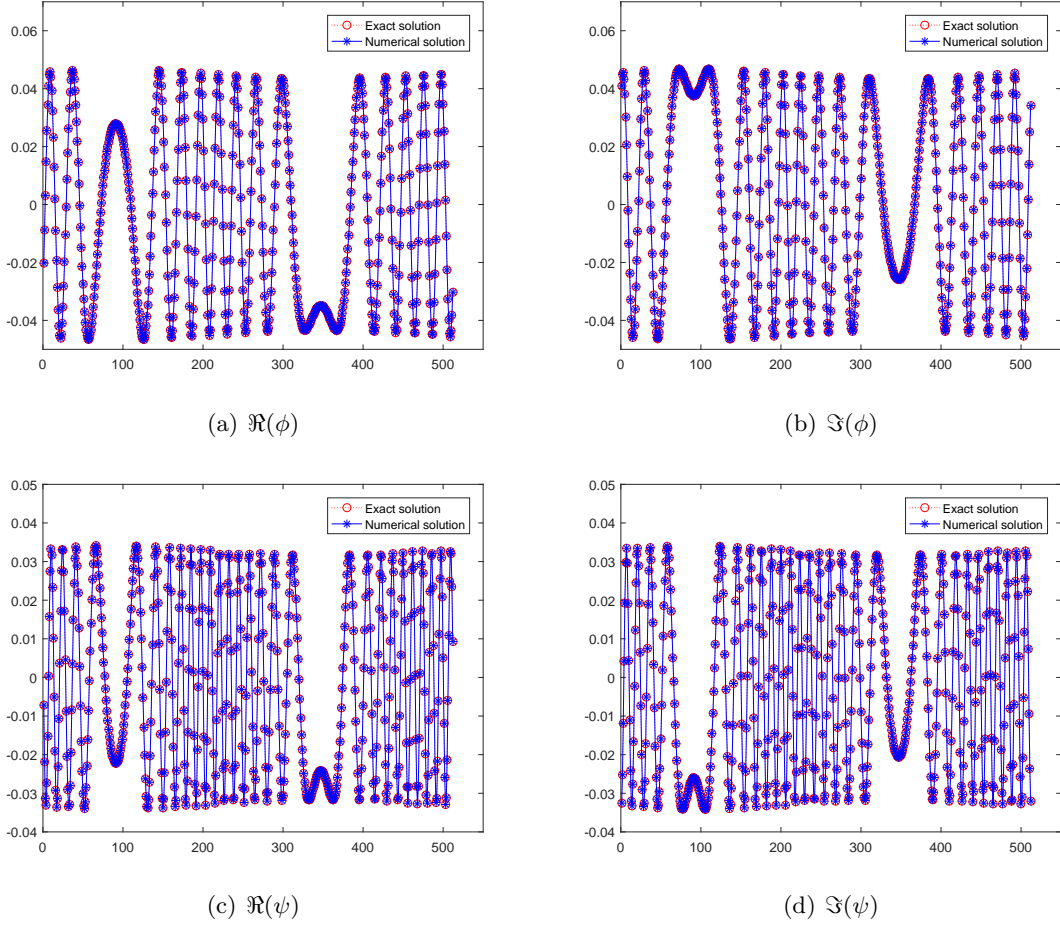


FIGURE 2. Numerical solutions and corresponding exact solutions for the apple-shaped obstacle with $\omega = 100\pi$, $n = \tilde{n} = 256$.

For the high-frequency case, we can get the same highly accurate results as those of the low-frequency case by increasing the number of interpolation points. The numerical solution and the corresponding exact solution are shown in Figure 2 for the apple-shaped obstacle with $\omega = 100\pi$. As can be seen, the numerical solutions and the exact solutions also coincide perfectly when $n = \tilde{n} = 256$.

It is worth mentioning that for a given incident wave and elastic obstacle, in view of (2.5) and (3.5), together with (5.4), we can get the compressional and shear far-field patterns immediately by using the trapezoidal rule. With the aid of (2.2), (3.1) and (5.4), noting $\mathbf{v}_p = \nabla\phi$ and $\mathbf{v}_s = \mathbf{curl}\psi$, we can also easily obtain the compressional and shear elastic scattered fields by using the trapezoidal rule, too, if the test points are not too close to the boundary.

5.2. Numerical examples: nonsmooth obstacles. In this subsection, we assume that D has a single corner at x_0 and assume $\Gamma_D \setminus \{x_0\}$ to be analytic. The angle γ at the corner is supposed to satisfy $0 < \gamma < 2\pi$. Suppose that the corner point x_0 corresponds to the parameter $t = 0$ in the parametric representation of Γ_D . To test the accuracy of our method, we adopt the exact solutions in form of (5.5) with the point source located at $\bar{x} = (0.1, 0.2)^\top$ and $\bar{x} = (-0.5, 0.2)^\top$ for the drop-shaped and heart-shaped obstacles, respectively. The interior angles are $\gamma = \pi/2$ and $\gamma = 3\pi/2$ for the drop-shaped and heart-shaped obstacles, respectively. The parameterizations of these two boundary curves are also shown in Table 1. In addition, we consider the case that the obstacle is

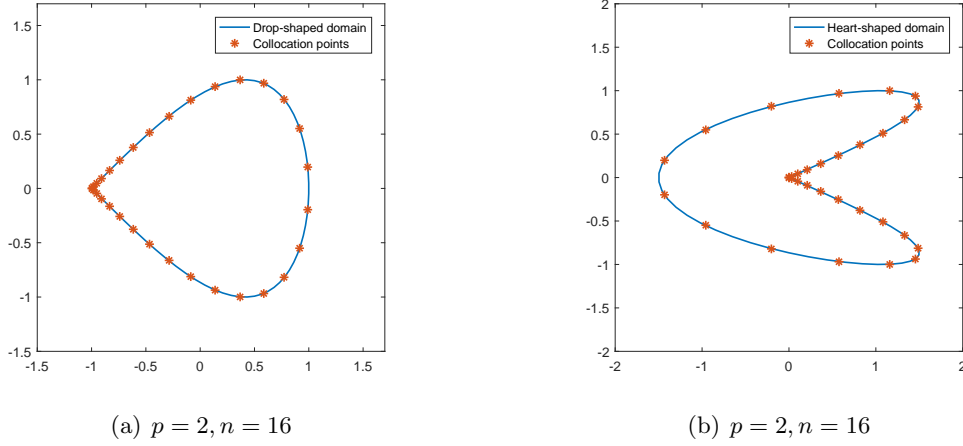


FIGURE 3. Collocation points on the drop-shaped and heart-shaped obstacles.

TABLE 4. Numerical errors for the drop-shaped domain with $\omega = \pi$.

n	Point source		Plane wave	
	$\ \phi_* - \phi^{(n)}\ _{L^2}$	$\ \psi_* - \psi^{(n)}\ _{L^2}$	$\ \phi^{(n_*)} - \phi^{(n)}\ _{L^2}$	$\ \psi^{(n_*)} - \psi^{(n)}\ _{L^2}$
16	2.0999e-03	2.1650e-03	4.5396e-01	5.8469e-01
32	2.4347e-08	3.1562e-08	3.9571e-03	4.9919e-03
64	1.2669e-08	1.6911e-08	2.7795e-04	3.7244e-04
128	3.8572e-10	5.1477e-10	2.4339e-05	2.8050e-05
256	1.1736e-11	1.5791e-11	1.1917e-04	1.6019e-04
512	1.3430e-14	1.7613e-14	9.2866e-06	1.2593e-05
1024	6.2155e-15	4.9608e-15	5.5606e-06	7.5428e-06
2048	6.1235e-15	5.9362e-15	1.1380e-07	1.5203e-07

TABLE 5. Numerical errors for the heart-shaped domain with $\omega = \pi$.

n	Point source		Plane wave	
	$\ \phi_* - \phi^{(n)}\ _{L^2}$	$\ \psi_* - \psi^{(n)}\ _{L^2}$	$\ \phi^{(n_*)} - \phi^{(n)}\ _{L^2}$	$\ \psi^{(n_*)} - \psi^{(n)}\ _{L^2}$
16	4.3673e-02	1.0523e-01	6.0929e-03	1.1896e-02
32	6.0075e-04	1.5144e-03	2.5014e-05	3.7337e-05
64	4.3721e-07	8.4011e-07	1.2432e-07	1.2820e-07
128	1.8692e-09	1.2039e-09	2.2355e-09	1.4398e-09
256	1.1752e-11	7.5236e-12	1.3571e-11	8.6880e-12
512	1.6306e-13	1.0433e-13	1.8443e-13	1.1843e-13
1024	4.5946e-15	4.0851e-15	8.0003e-15	5.9002e-15
2048	1.1742e-14	1.3828e-14	9.6079e-15	1.0804e-14

illuminated by a compressional plane wave \mathbf{u}^{inc} which is given by

$$\mathbf{u}^{\text{inc}}(x) = de^{i\kappa_p d \cdot x},$$

where $d = (\cos \theta, \sin \theta)^\top$ is the unit propagation direction vector.

To resolve the field near the corner, we adopt the graded mesh by taking the substitution [7, 15] $t = w(s)$, which is given by

$$w(s) = 2\pi \frac{[v(s)]^p}{[v(s)]^p + [v(2\pi - s)]^p}, \quad 0 \leq s \leq 2\pi,$$

where

$$v(s) = \left(\frac{1}{p} - \frac{1}{2}\right) \left(\frac{\pi - s}{\pi}\right)^3 + \frac{1}{p} \frac{s - \pi}{\pi} + \frac{1}{2}, \quad p \geq 2,$$

and is applied to the parametric curve of the drop-shaped and heart-shaped obstacles. In experiments, we choose $s_j := \pi j/n + \pi/(2n)$ as the collocation points in (5.4). The generated points $w(s_j)$, $j = 0, \dots, 2n - 1$ of the graded mesh on the both boundaries are presented in Figure 3 for $p = 2$.

The numerical errors between the numerical solution and the exact solution (5.5) with $L^2(\partial B)$ norm for the drop-shaped and heart-shaped obstacles are listed in Tables 4 and 5 with the angular frequency $\omega = \pi$ and $\tilde{n} = 16$. Additionally, we calculate the values of compressional and shear scattered fields $\phi^{(n_*)}, \psi^{(n_*)}$ on ∂B with $\tilde{n} = 16, n_* = 4096$ by the incident plane wave with $\theta = \pi/6$, and compare them with the cases of other numbers of collocation points. For the point source case, the solver quickly converges to machine precision for both domains. This is due to the analyticity of the artificial solution. On the other hand, for the true scattering problem, i.e., the scattering problem of the plane wave incidence, we note that the numerical error of the heart-shaped domain is better than that of the drop-shaped domain. The reason is apparently related to the concavity of the domain. Detailed analysis will be investigated in the future work.

6. CONCLUSION

We have proposed a novel boundary integral formulation and developed a highly accurate numerical method for solving the time-harmonic elastic scattering from a rigid bounded obstacle immersed in a homogeneous and isotropic elastic medium. Using the Helmholtz decomposition, we reduce the scattering problem to a coupled boundary integral equation with singular integral operators. By introducing an appropriate regularizer to the coupled system, we split the operator equation in the form of an isomorphic operator plus a compact one. The convergence is shown for both the semi-discrete and full-discrete schemes via the trigonometric collocation method. Numerical experiments for smooth and nonsmooth obstacles, especially for the obstacles with corners, are presented to demonstrate the superior performance of the proposed method. Along this line, we intend to extend the current work to the coupled fluid-solid scattering problem and the three-dimensional elastic obstacle scattering problem, where the more complicated model equations need to be considered.

REFERENCES

- [1] J. F. Ahner and G. C. Hsiao, On the two-dimensional exterior boundary-value problems of elasticity, *SIAM J. Appl. Math.*, 31 (1976), 677–685.
- [2] B. Alpert, Hybrid Gauss-trapezoidal quadrature rules, *SIAM J. Sci. Comput.*, 20 (1999) 1551–1584.
- [3] H. Ammari, E. Bretin, J. Garnier, H. Kang, H. Lee, and A. Wahab, *Mathematical Methods in Elasticity Imaging*, Princeton University Press, New Jersey, 2015.
- [4] A. Anand, J. Owall, and C. Turc, Well conditioned boundary integral equations for two-dimensional sound-hard scattering problems in domains with corners, *J. Integral Equ. Appl.*, 24 (2012), 1–38.
- [5] G. Bao, L. Xu, and T. Yin, An accurate boundary element method for the exterior elastic scattering problem in two dimensions, *J. Comput. Phys.*, 348 (2017), 343–363.
- [6] F. Bu, J. Lin, and F. Reitich, A fast and high-order method for the three-dimensional elastic wave scattering problem, *J. Comput. Phys.*, 258 (2014), 856–870.
- [7] D. Colton and R. Kress, *Inverse Acoustic and Electromagnetic Scattering Theory*, 3rd edition, Springer, New York, 2013.
- [8] H. Dong, J. Lai, and P. Li, Inverse obstacle scattering for elastic waves with phased or phaseless far-field data, *SIAM J. Imaging Sci.*, 12 (2019), 809–838.

- [9] H. Dong, J. Lai, and P. Li, An inverse acoustic-elastic interaction problem with phased or phaseless far-field data, *Inverse Probl.*, 36 (2020), 035014.
- [10] D. Givoli and J. B. Keller, Non-reflecting boundary conditions for elastic waves, *Wave Motion*, 12 (1990), 261–279.
- [11] L. Greengard and S. Jiang, A new mixed potential representation for the equations of unsteady, incompressible flow, *SIAM Review*, 61 (2019), 733–755.
- [12] G. Hu, A. Kirsch, and M. Sini, Some inverse problems arising from elastic scattering by rigid obstacles, *Inverse Problems*, 29 (2013), 015009
- [13] A. Kirsch, *An Introduction to the Mathematical Theory of Inverse Problems*, 2nd edition, Springer, New York, 2011.
- [14] A. Kirsch and S. Ritter, The Nyström method for solving a class of singular integral equations and applications in 3D-plate elasticity, *Math. Meth. Appl. Sci.*, 22 (1999), 177–197.
- [15] R. Kress, A Nyström method for boundary integral equations in domains with corners, *Numer. Math.*, 58 (1990), 145–161.
- [16] R. Kress, On the numerical solution of a hypersingular integral equation in scattering theory, *J. Comput. Appl. Math.*, 61 (1995), 345–360.
- [17] R. Kress, A collocation method for a hypersingular boundary integral equation via trigonometric differentiation, *J. Integral Equ. Appl.*, 26 (2014), 197–213.
- [18] R. Kress, *Linear Integral Equations*, 3rd edition, Springer, New York, 2014.
- [19] R. Kress and I. H. Sloan, On the numerical solution of a logarithmic integral equation of the first kind for the Helmholtz equation, *Numer. Math.*, 66 (1993), 199–214.
- [20] J. Lai and P. Li, A framework for simulation of multiple elastic scattering in two dimensions, *SIAM J. Sci. Comput.*, 41 (2019), A3276–A3299.
- [21] L. D. Landau and E. M. Lifshitz, *Theory of Elasticity*, Oxford: Pergamon 1986.
- [22] F. Le Louër, On the Fréchet derivative in elastic obstacle scattering, *SIAM J. Appl. Math.*, 72 (2012), 1493–1507.
- [23] F. Le Louër, A high order spectral algorithm for elastic obstacle scattering in three dimensions, *J. Comput. Phys.*, 279 (2014), 1–17.
- [24] S. G. Mikhlín and S. Prössdorf, *Singular Integral Operators*, Springer Verlag, Berlin, 1986.
- [25] Y. H. Pao and V. Varatharajulu, Huygens’ principle, radiation conditions, and integral formulas for the scattering of elastic waves, *J. Acoust. Soc. Amer.*, 59 (1976), 1361–1371.
- [26] J. Saranen and G. Vainikko, Trigonometric collocation methods with product integration for boundary integral equations on closed curves, *SIAM J. Numer. Anal.*, 33 (1996), 1577–1596.
- [27] M. S. Tong and W. C. Chew, Nyström method for elastic wave scattering by three-dimensional obstacles, *J. Comput. Phys.*, 226 (2007), 1845–1858.
- [28] J. Yue, M. Li, P. Li, and X. Yuan, Numerical solution of an inverse obstacle scattering problem for elastic waves via the Helmholtz decomposition, *Commun. Comput. Phys.*, 26 (2019), 809–837.

SCHOOL OF MATHEMATICS, JILIN UNIVERSITY, CHANGCHUN, JILIN 130012, CHINA

E-mail address: dhp@jlu.edu.cn

SCHOOL OF MATHEMATICAL SCIENCES, ZHEJIANG UNIVERSITY, HANGZHOU, ZHEJIANG 310027, CHINA

E-mail address: laijun6@zju.edu.cn

DEPARTMENT OF MATHEMATICS, PURDUE UNIVERSITY, WEST LAFAYETTE, INDIANA 47907, USA

E-mail address: lipeijun@math.purdue.edu